Regular Article

PHYSICAL CHEMISTRY RESEARCH
Published by the
Iranian Chemical Society
www.physchemres.org
info@physchemres.org

Phys. Chem. Res., Vol. 8, No. 2, 313-341, June 2020
DOI: DOI: 10.22036/pcr.2020.212523.1709

Response Surface Methodology (RSM) for Statistical Optimization of Cd^{2+} Removal Using Modified Zn_2Al-layer Double Hydroxide by Quinoline Yellow

M. Janighorban[a], N. Sohrabi[b,*], N. Rasouli[c,*] and M. Ghaedi[d]

[a,b,c]*Department of Chemistry, Payame Noor University, P. O. Box: 19395-3697, Tehran, Iran*

[d]*Chemistry Department, Yasouj University, Yasouj 75918-74831, Iran*

(Received 19 December 2019, Accepted 12 March 2020)

Modified Zn_2Al-layered double hydroxide (LDH) intercalated with quinoline yellow (Q) (Zn_2Al-LDH/Q) was prepared by a facile and simple method and then used to remove of Cd^{2+} ions from water. The chemical composition and morphology of Zn_2Al-LDH/Q were investigated by X-ray diffraction (XRD), Brunauer-Emmett-Teller (BET), field emission scanning electron microscopy (FE-SEM) and energy-dispersive X-ray spectroscopy. Response surface methodology was employed to optimize the adsorption parameters of Cd^{2+}. Such optimization was undertaken to ensure a high efficiency over the experimental ranges employed and to evaluate the interactive effects of the initial concentration of Cd^{2+}, pH, adsorbent dosage, temperature and contact time in order to improve the conditions employed in the batch process. The analysis of variance (ANOVA) indicated that a second-order polynomial regression equation was the most appropriate polynomial for fitting the experimental data. The experimental confirmation tests showed a correlation between the predicted and experimental responses (R^2). The optimum adsorption parameters were predicted as an initial Cd^{2+} concentration of 35 mg l^{-1}, a pH value of 4.17, the adsorbent dosage of 0.03 g l^{-1}, a temperature of 32.5 °C and contact time of 51 min. Under optimum conditions, the highest adsorption efficiency and maximum adsorption capacity were 45% and 12.18 mg g^{-1}, respectively.

Keywords: Layered double hydroxide, Cd^{2+}Adsorption, Response surface methodology, Quinoline yellow

INTRODUCTION

The elimination of heavy metals from water is very important from environmental and human health viewpoints [1,2]. In this regard, Cd(II) is a major environmental problem because of its potential agglomeration, non-biodegradability, and high toxicity in ecosystems and human bodies [3]. The allowable limit for Cd in drinking water is set at 3.0 ppb by World Health Organization (WHO) [4]. Moreover, the supply of Cadmium in human bodies can cause persistent disorders of the liver, kidney and nervous systems [5]. The available technologies for the elimination of heavy metals from wastewater include chemical precipitation, ion exchange, membrane filtration and adsorption [6-11]. However, most of these methods have high cost, average removal efficiency and take multiple long steps to complete process [12]. In this regard, adsorption is proved to be the more efficient process due to its low cost, higher uptake potential, high selectivity, low production of sludge and easy operation [13-17]. Layered double hydroxides (LDHs) or hydrotalcite-like compounds known as the anionic clay have become an important type of adsorbents owing to its efficient adsorption and reusability. Layered double hydroxides have the general formula $[M_{1-x}^{II}M_x^{III}(OH)_2]_x^+[A_n]^{x/n}.mH_2O$, where M^{II} and M^{III} stand for a divalent and a trivalent cation, respectively, A_n is the interlayer anion, such as CO_3^{2-}, Cl^- and NO_3^- located in the interlayer and the lamellar surface. Also, layered double hydroxide materials have gained many potential applications such as super capacitors [18, 19], catalysis [20,21], drug delivery [22,23] wastewater

*Corresponding authors. E-mail: sohrabnas@pnu.ac.ir; n.rasooli55@yahoo.com

treatment [24-27] and flame retardant epoxy formulation [28]. Especially, their applications as adsorbents have attracted a great attention due to their low cost, high surface area, highly tunable interior architecture [29], non-toxicity [30,31] and exchangeable anionic properties [32]. In this regard, LDHs have been modified in various forms in order to improve their adsorption capacity [33,34]. Previous studies demonstrated that LDHs intercalated with amino acids [35], ethylene diamine tetra acetic acid [36], glutamate [37], and diethylene tri-amine penta acetate and meso-2,3-dimercaptosuccinate [38], possessed a higher affinity to potentially toxic metal cations than the pristine LDH adsorbents. Efforts have been made to improve the adsorption capacity of these materials for heavy metal removal. The adsorption capacity of an adsorbent depends strongly on various factors such as pH value of solution, contact time, temperature, and adsorbent dose [39]. Conventional methods for investigating the adsorption process are usually conducted by changing one independent variable and keeping the other factors constant. However, in this case, the obtained results cannot reveal the combined effect of all the factors involved simultaneously. Additionally, such methods are often time consuming and require a number of experiments which are unreliable to determine optimum levels. Therefore, response surface methodology (RSM), based on the statistical experimental design, has been widely used to eliminate the limitations of single factor experiments by optimizing all the influencing factors collectively. In this work, quinoline yellow (Scheme 1) was used for the modification of Zn_2Al-LDH to enhance the adsorption capacity for Cd^{2+} adsorption.

MATERIALS AND INSTRUMENTATION

All materials were commercial reagent grade and purchased from Merck and Sigma Aldrich. The Cd^{2+} concentration was determined using atomic absorption spectrometer, Specter AA 220, VARIAN. Magnetic stirrer and water bath used were IKA, big-squid [ocean], and Julabo F12-MP, (from Germany), respectively. The analysis of the samples was performed by powder X-ray diffraction (Holland Philips X-pert, X-ray diffractometer with Cu-Kα radiation). The particle size, external morphology and analysis of elements in the samples were characterized by scanning electron microscopy (JEOL JEM-3010 SEM) and the BET analysis was performed using BELSORP Mini II instrument. A digital pH meter (InoLab pH 730, Germany) was employed for adjusting pH.

Preparation of Zn_2Al-LDH Intercalated with Quinoline Yellow (Q)

Modified Zn_2Al-layered double hydroxide (LDH) intercalated with quinoline yellow (Q) (Zn_2Al-LDH/Q) was prepared through co-precipitation method [40]. Firstly, carbon dioxide free (CO_2-free) solution was prepared by flowing N_2 into deionized water for 30 min at 60 °C, and used throughout the preparation process. In a typical procedure, a mixture of $Zn(NO_3)_2.6H_2O$ (5.8 g, 0.018 mol) and $Al(NO_3)_3.9H_2O$ (3.2 g, 0.008 mol) with Al to Zn molar ration (1:2) and quinoline yellow (7.7 g, 0.028 mol) in 250 ml deionized water was added to a solution of NaOH (1 M) under constant stirring until reaching pH = 10-11, then continue flowing N_2 in solution at 60 °C to complete precipitation process. Then, the obtained product was stirred for 24 h at 65 ºC (Scheme 2). After several times filtration and washing with distilled water, the solid product was dried at room temperature.

Adsorption Studies

The Cd^{2+} concentrations were determined according to general traditional flame atomic absorption spectrometry, at 228.8 nm wavelength, standard working concentration range: 0.25-0.5-1.0 and fuel acetylene. The efficiency of Cd^{2+} removal was determined at different experimental conditions specified according to CCD method. The adsorption capacity for Cd^{2+} uptake, q_e (mg g^{-1}), at equilibrium, can be determined by the following Eq. (1):

$$q_e = \frac{(C_i - C_e)V}{m} \quad (1)$$

where C_i and C_e (mg l^{-1}) refer to cadmium concentrations at initial and equilibrium conditions, respectively, V (l) is the cadmium solution volume, and m (g) is the adsorbent mass.
In the kinetic study, Cd^{2+} adsorption amount (q_t) can be calculated by Eq. (2):

$$q_t = \frac{(C_0 - C_t)}{C_0} \times 100 \quad (2)$$

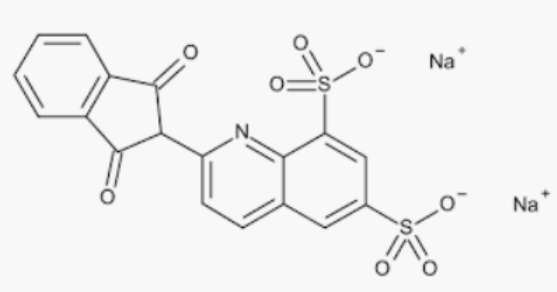

Scheme 1. The chemical structure of quinoline yellow

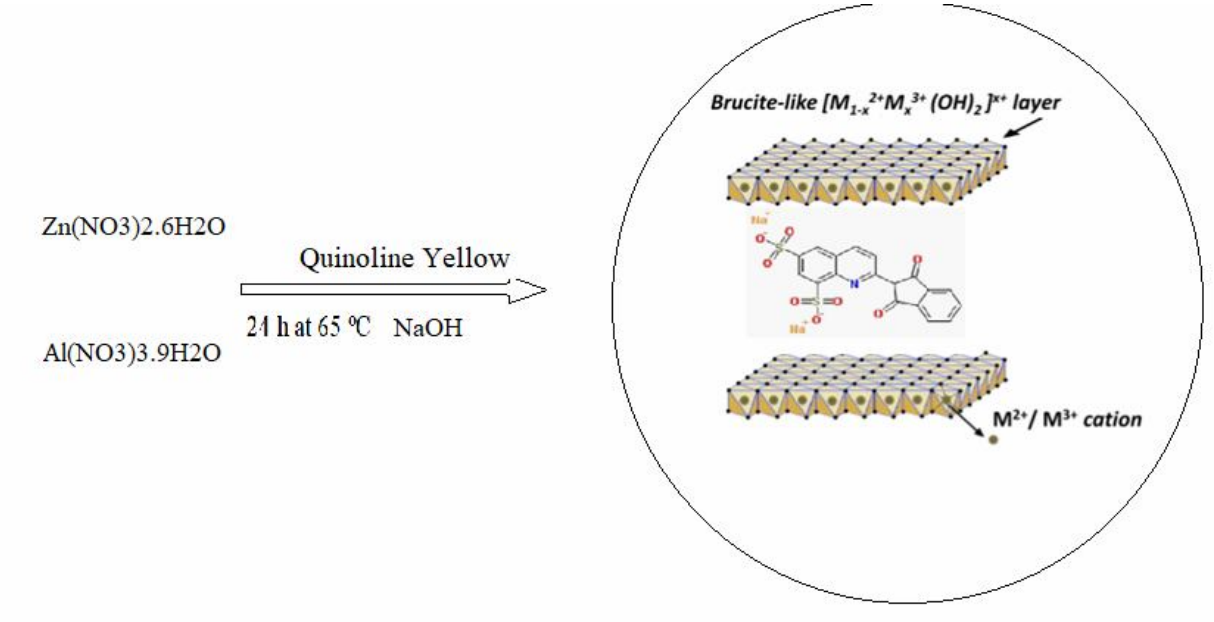

Scheme 2. Schematic of Zn_2Al-LDH/Q preparation

where C_i and C_t (mg l^{-1}) are Cd^{2+}concentration at initial and time t, respectively, V (l) is the Cd^{2+} solution volume, and m (g) is the Zn_2Al-LDH/Q adsorbent mass.

Central Composite Design (CCD)

In this work, according to RSM design, CCD was used to assess the effect of adsorption conditions on the efficiency of Cd^{2+} removal. The effect of Cd^{2+} concentration (A), pH (B), adsorbent mass (C), contact time (D) and temperature bath (E) on adsorption efficiency was optimized using 5 factors at 5 levels (-α, -1, 0, +1, +α) based on CCD in Table 1.

The collected number of 32 experiments containing 6 replicates at the center point was applied to find mathematical correlate among the independent variable and the corresponding response values. The statistical software Design Expert V.7.1.5 was applied to analyze the experimental data and generate a second-order polynomial model.

RESULTS AND DISCUSSION

Characterization of Adsorbent

The crystal structures and phase purity of the

Table 1. The Levels of Factors in CCD

Factors	Unit	Symbol	levels					
			-α	Low actual	Mean	High actual	+α	Std. Dev.
Concentration (C)	mg l^{-1}	A	-1	35.00	57.500	80.00	+1	19.486
pH		B	-1	4.00	6.500	9.00	+1	2.165
Adsorbent mass (m)	g l^{-1}	C	-1	0.027	0.046	0.064	+1	0.016
Contact time (time)	min	D	-1	35.00	60.00	85.00	+1	21.651
Temperature (T)	°C	E	-1	20.00	30.00	40.00	+1	8.660

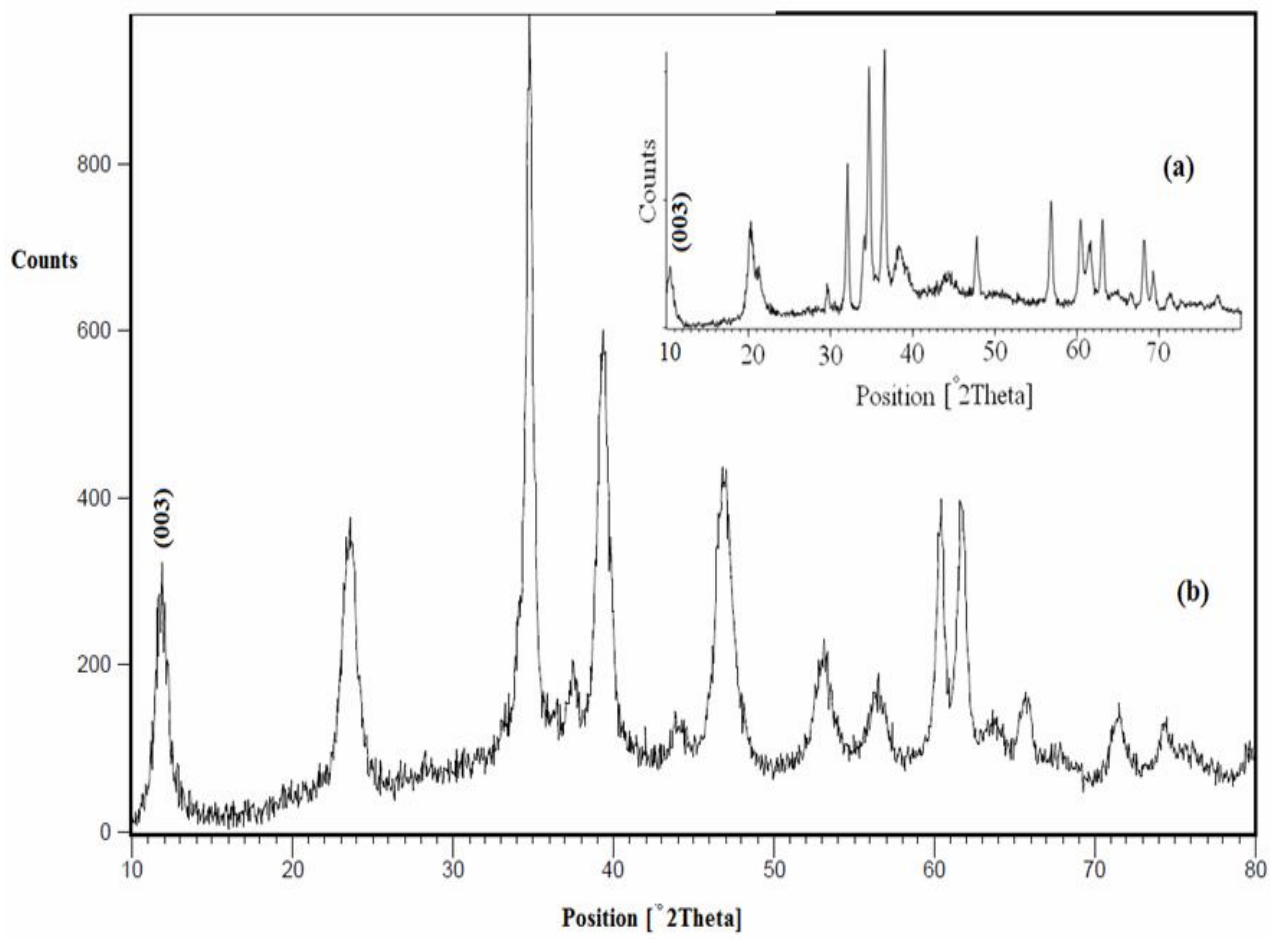

Fig. 1. XRD images of (a) Zn_2Al-LDH, (b) Zn_2Al-LDH/Quinoline Yellow.

synthesized Zn_2Al-LDH/Q have been investigated by XRD. Figure 1 shows the XRD pattern of Zn_2Al-LDH/Q. The results showed that the synthesized Zn_2Al-LDH/Q exhibits typical characteristics of LDH phase (Fig. 1) [41]. The peaks in the XRD pattern of Zn_2Al-LDH/Q are similar to those of Zn_2Al-LDH. However, compared to Zn_2Al-LDH, the (003) diffraction peak of Zn_2Al-LDH/Q moves to the bigger 2θ angle of 11.77 and the basal spacing decreased to 0.75 nm. This result can confirm intercalation of quinoline yellow by the anion exchange in the Zn_2Al-LDH compound [42]. The crystallite sizes for the synthesized Zn_2Al-LDH/Q were calculated using Scherer formula (Eq. (3)):

$$D = \frac{0.9\lambda}{\beta \cos\theta} \tag{3}$$

where λ is the wavelength of X-ray, β is full width at half maximum of the peak at diffracting angle θ. The calculated crystallite sizes were 24 nm.

The morphology and chemical composition of the synthesized sample were investigated by FE-SEM and EDS. The FE-SEM images of the synthesized sample are shown in Fig. 2. The original sheet and lamellar structure of Zn_2Al-LDH changed over intercalation of quinoline yellow. The EDS spectrum of the prepared sample (Fig. 3) shows the presence of relevant elements, demonstrating purity of the synthesized Zn_2Al-LDH/Q.

The adsorption method of Brunauer, Emmett and Teller (BET) is based on the physical adsorption of a vapour or gas onto the surface of a solid. Such data can be used to analyse the porosity of the materials being studied. In this research, the BET method was used. The interference by the surrounding phase is especially problematic for the Bruner–Emmet-Teller (BET) N_2 adsorption/desorption isotherm method, because the entire surface is modified by vacuum treatment before N_2 adsorption. From Table 2 and Fig. 4, it can be observed that sorbent seems to posses an appreciable narrow micro-porosity. The total surface properties of the adsorbent are presented in Table 3.

CCD Analysis

The most important variables and their influence on response and main interaction with other variables were investigated by analysis of variance (ANOVA) using STATISTICA 10. The optimal conditions for the removal percentage of Cd^{2+} (responses) were determined using the optimal model predict or linear factors equation. Subsequently, analysis of variance (ANOVA) and their comparison with statistical reference value in Table 3 were performed to ensure the adequacy of the proposed model. Also, quality of obtained results was expressed based on the predicated R^2 value. The statistical analysis included the estimated regression coefficients and p-values. The obtained p-values for more terms were less than 0.05 (95% confidence interval), indicating their significance. Also, the absence of Fit F-value 3.63 for Zn_2Al-LDH/Q could be a good indication of suitability of the model for fitting experimental data and optimization points in Table 4 and Table 5, respectively.

Moreover, the most effective parameters were determined based of p- and F-values. The below empirical relationship between the response and independent variables as the Linear equation is applicable to predict real behavior of the adsorption system at the various conditions.

$$\begin{aligned}\%\text{Efficiency} = {} & +4.73277 - 0.28115 \times C + 5.97567 \times pH \\ & + 216.34964 \times m - 0.10410 \times time \\ & + 0.88442 \times T \end{aligned} \tag{4}$$

Generally, when the coefficient of each parameter becomes high, it confirms a highly positive influence on the response. The negative value of each parameter shows that there is a reverse correlation between responses and the parameter, meaning that the negative value results in the achievement of maximum responses. According to this equations, pH, amount of adsorbent and temperature bath have a positive effect, and time and concentration of Cd^{2+} have a negative effect on yield process (removal percentage of Cd^{2+}). As can be shown from these equations, the factor of pH, amount of adsorbent and temperature bath have the most positive effect on the removal percentage of Cd^{2+}. It means that with increasing the adsorbent dosage, the removal of Cd^{2+} increases.

Optimization of Conditions

The linear model was suggested by the software for yield. ANOVA data (Table 5) shows that the model F-value

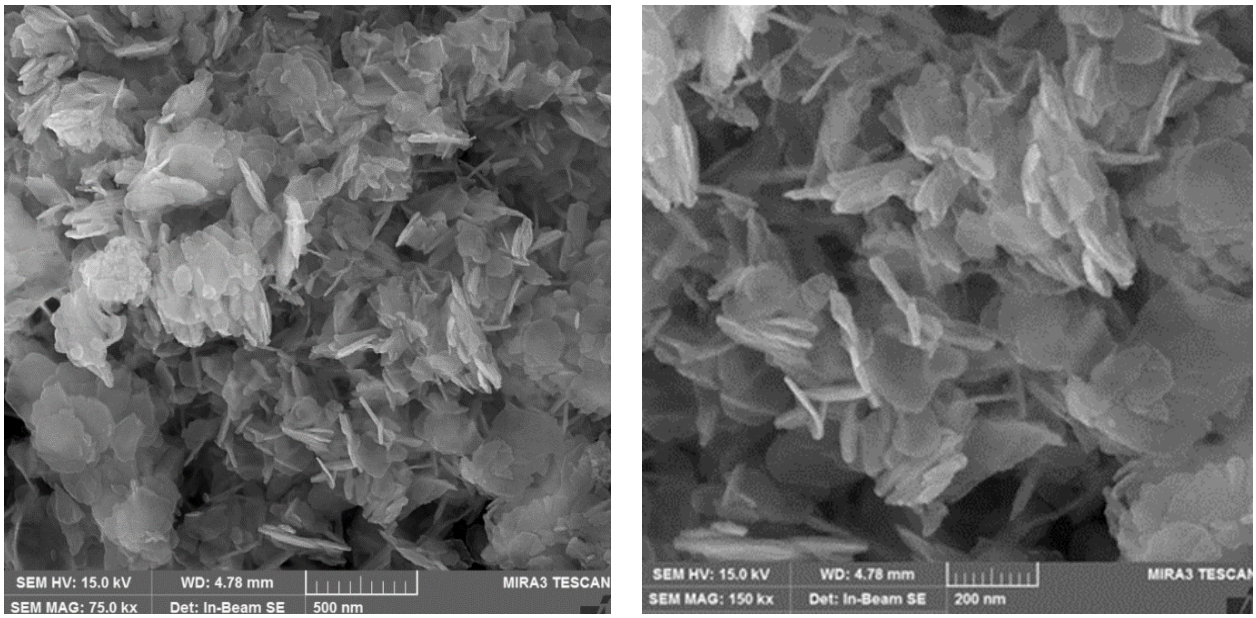

Fig. 2. The FE-SEM images of (a) Zn_2Al-LDH, and (b) Zn_2Al-LDH/Q.

Table 2. Surface Area and Porosity Measurement (BET Method) of Zn_2Al-LDH/Q

Sample	Surface area ($m^2\ g^{-1}$)	Micropore Vol. ($cc\ g^{-1}$)	Micropore size (nm)
Zn_2Al-LDH/Q	33.725	0.2409	28.578

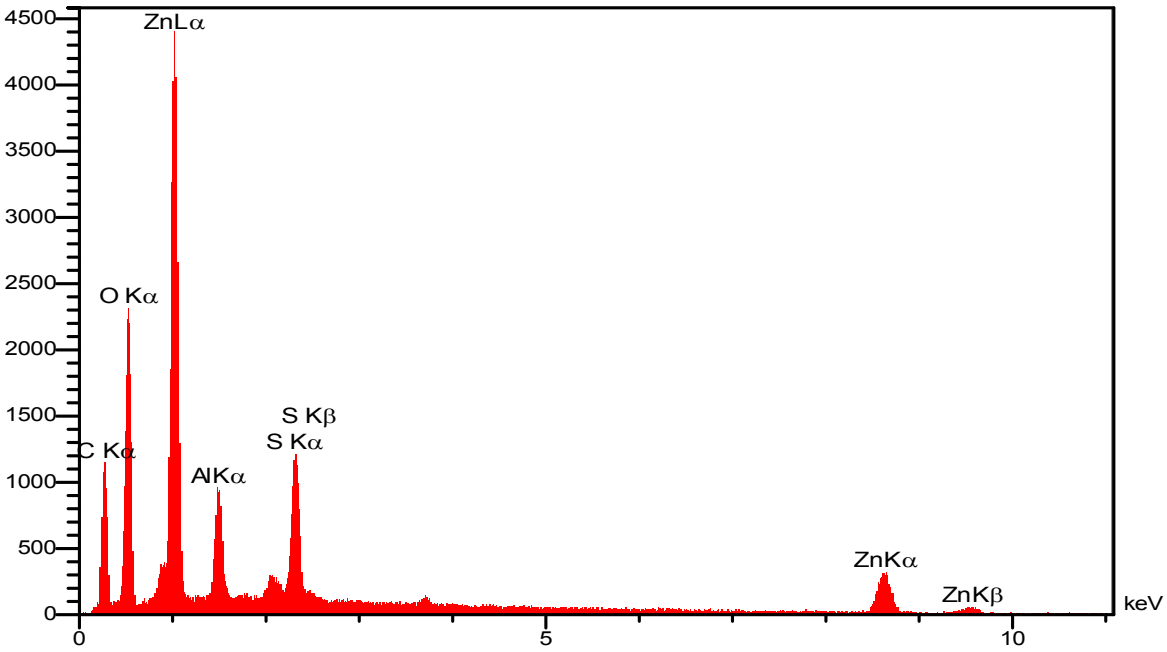

Fig. 3. The EDS image of Zn_2Al-LDH/Q.

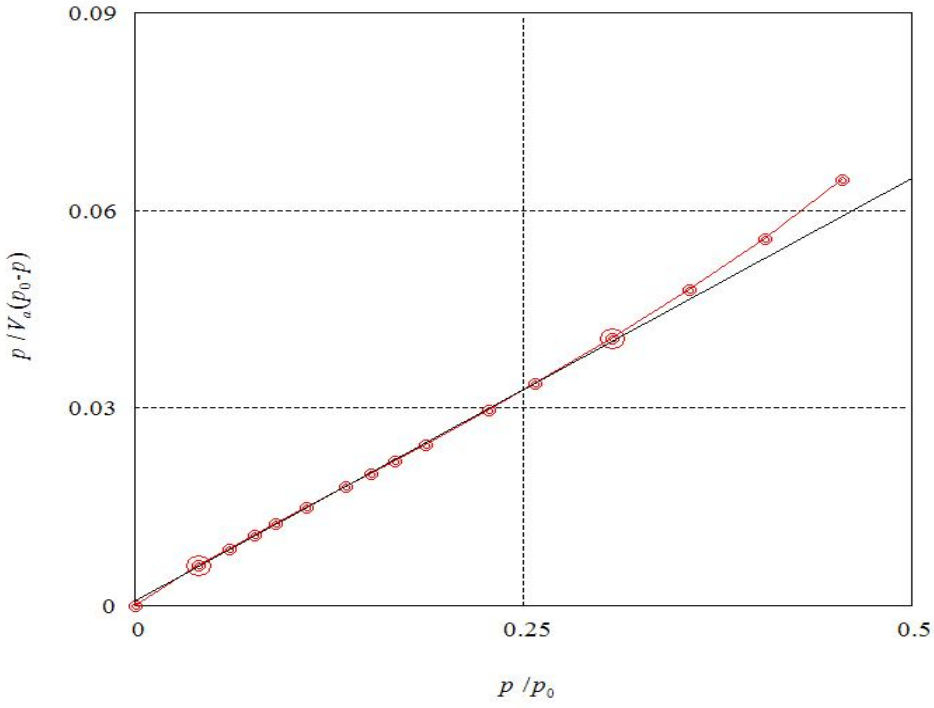

BET-Plot

Adsorptive N2

Adsorption temperature77.000[K]

Fig. 4. The BET images of Zn_2Al-LDH/Q.

Table 3. The Matrix Design and the Responses

Run	A	B	C	D	E	%Efficiency	q_e
1	35	9	0.06	35	40	87.79	1.98
2	80	4	0.03	85	40	29.1	9.58
3	35	9	0.06	85	20	85.8	1.97
4	35	4	0.06	85	40	89.86	12.31
5	57.5	6.5	0.05	60	30	29.02	7.30
6	35	4	0.03	85	20	21.64	4.26
7	80	4	0.03	35	20	23.38	7.11
8	57.5	6.5	0.05	60	30	32.47	8.25
9	57.5	6.5	0.05	60	30	33.8	8.75
10	35	4	0.06	35	20	12.92	1.28
11	57.5	6.5	0.05	60	50	73.76	14.79
12	57.5	6.5	0.05	60	30	33.8	8.75
13	80	9	0.03	85	20	84.43	4.35
14	57.5	6.5	0.05	60	10	42.39	10.86
15	80	9	0.03	35	40	91.79	3.18
16	57.50	6.50	0.05	60	30	54.8	13.98
17	80	4	0.06	85	20	30.7	4.42
18	57.5	6.5	0.05	110	30	71.06	14.28
19	57.5	1.5	0.05	60	30	11.45	4.08
20	35	4	0.03	35	40	99.13	24.8
21	12.5	6.5	0.05	60	30	76.11	4.01
22	57.5	11.5	0.05	60	30	71.36	1.22
23	102.5	6.5	0.05	60	30	50.98	21.18
24	57.5	6.5	0.08	60	30	79.51	8.39
25	57.5	6.5	0.05	60	30	49.25	12.59
26	35	9	0.03	35	20	59.74	3.19
27	57.5	6.5	0.01	60	30	50.20	59.54
28	80	9	0.06	85	40	100	1.48
29	57.5	6.5	0.05	10	30	45.38	9.16
30	35	9	0.03	85	40	97.37	5.3
31	80	4	0.06	35	40	37.74	5.56
32	80	9	0.06	35	20	100	2.14

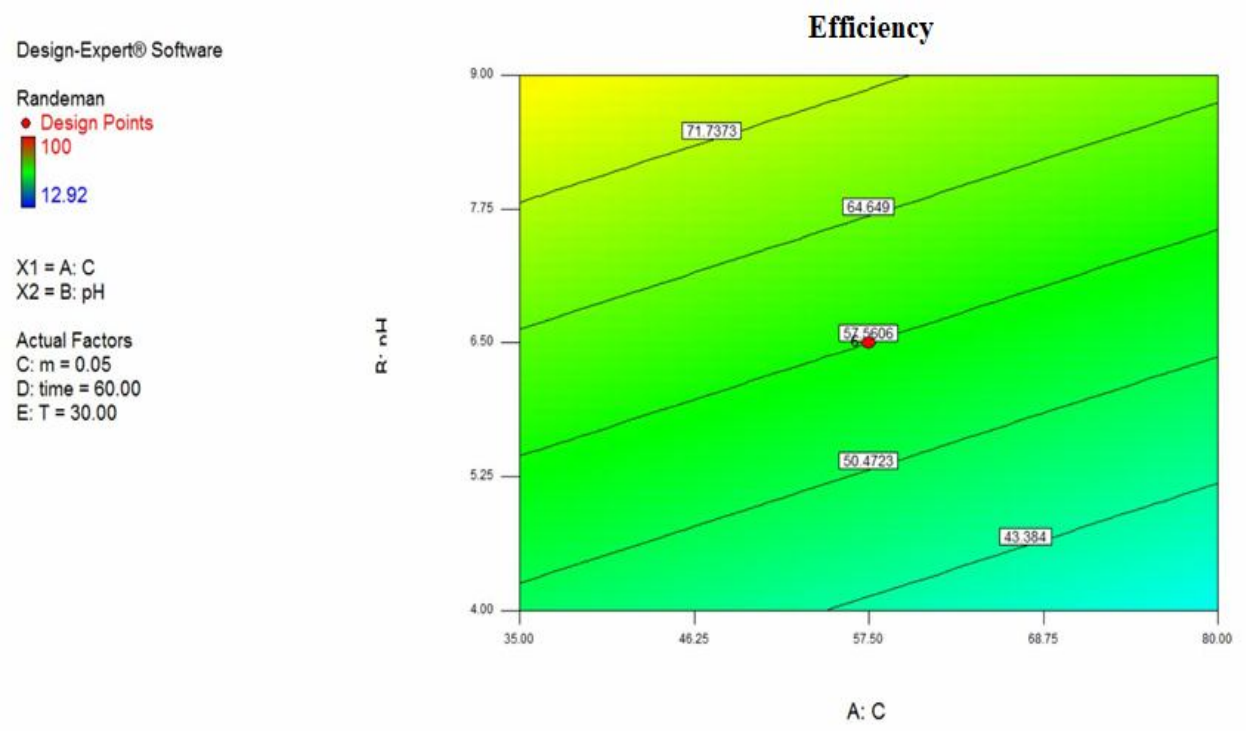

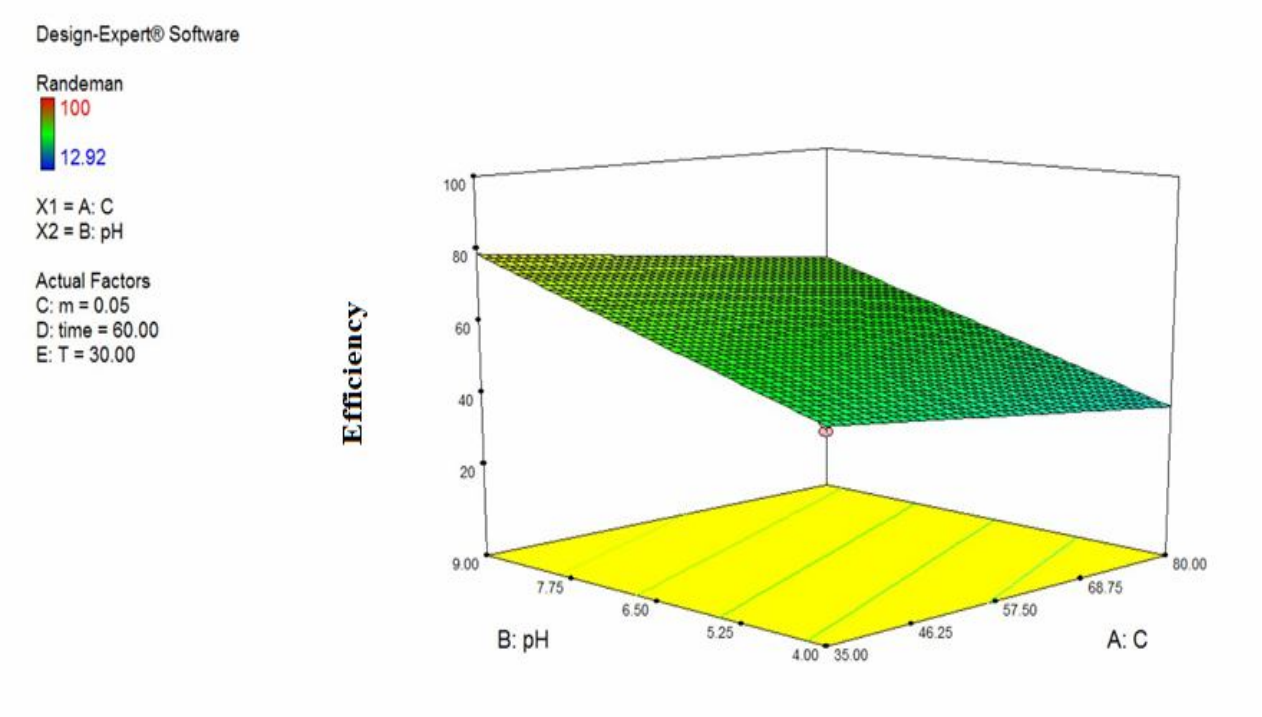

(a)

Fig. 5. The 3D surfaces and contour plots for interactive effect variables.

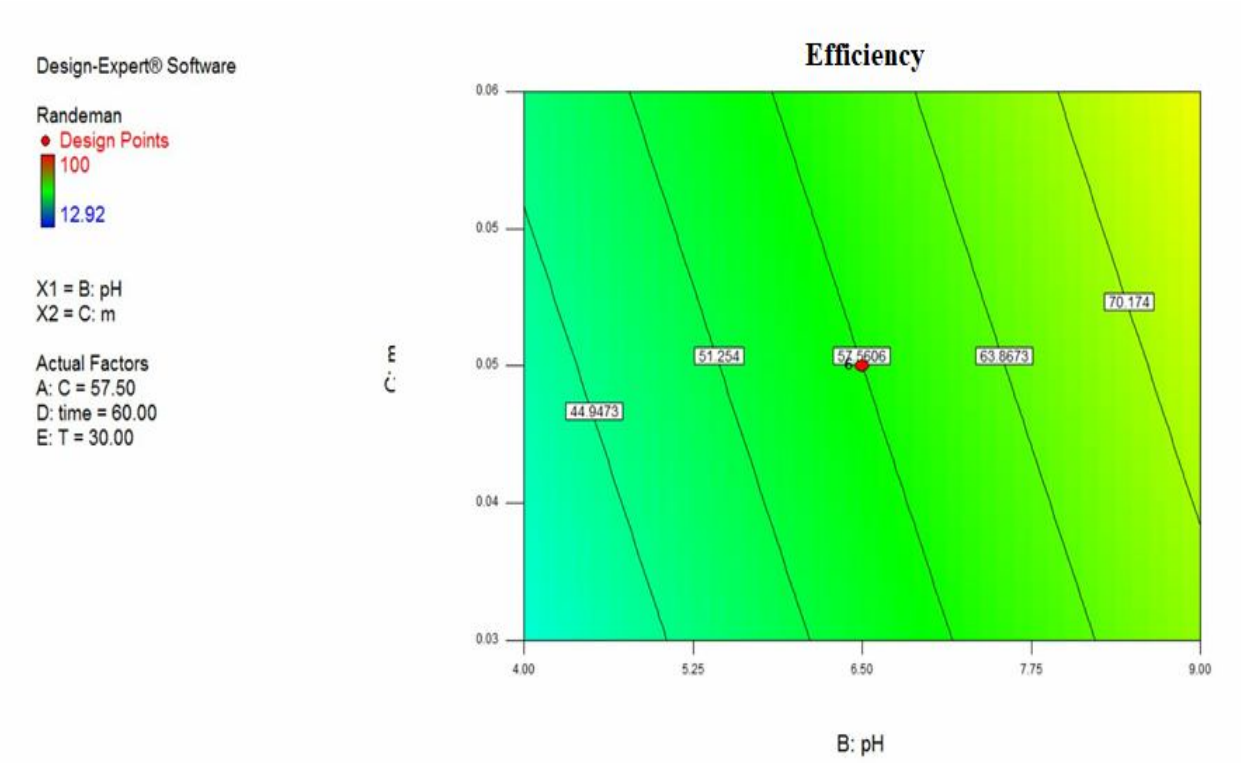

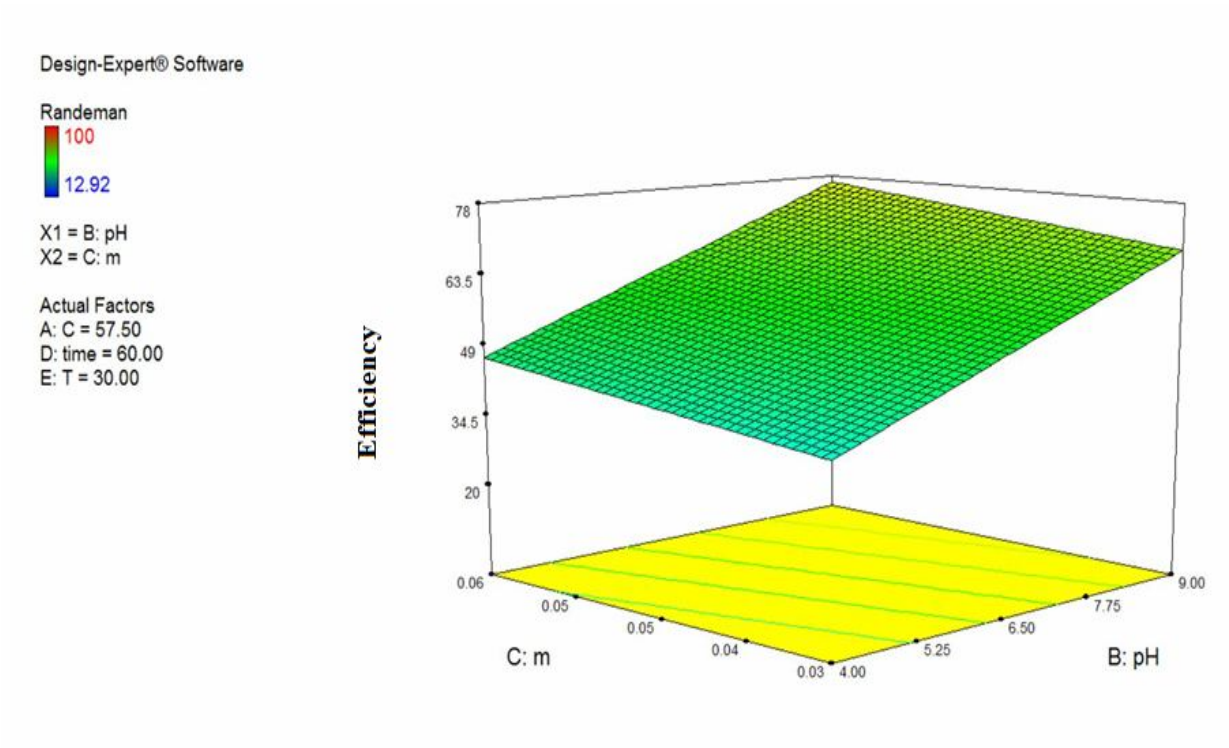

(b)

Fig. 5. Continued.

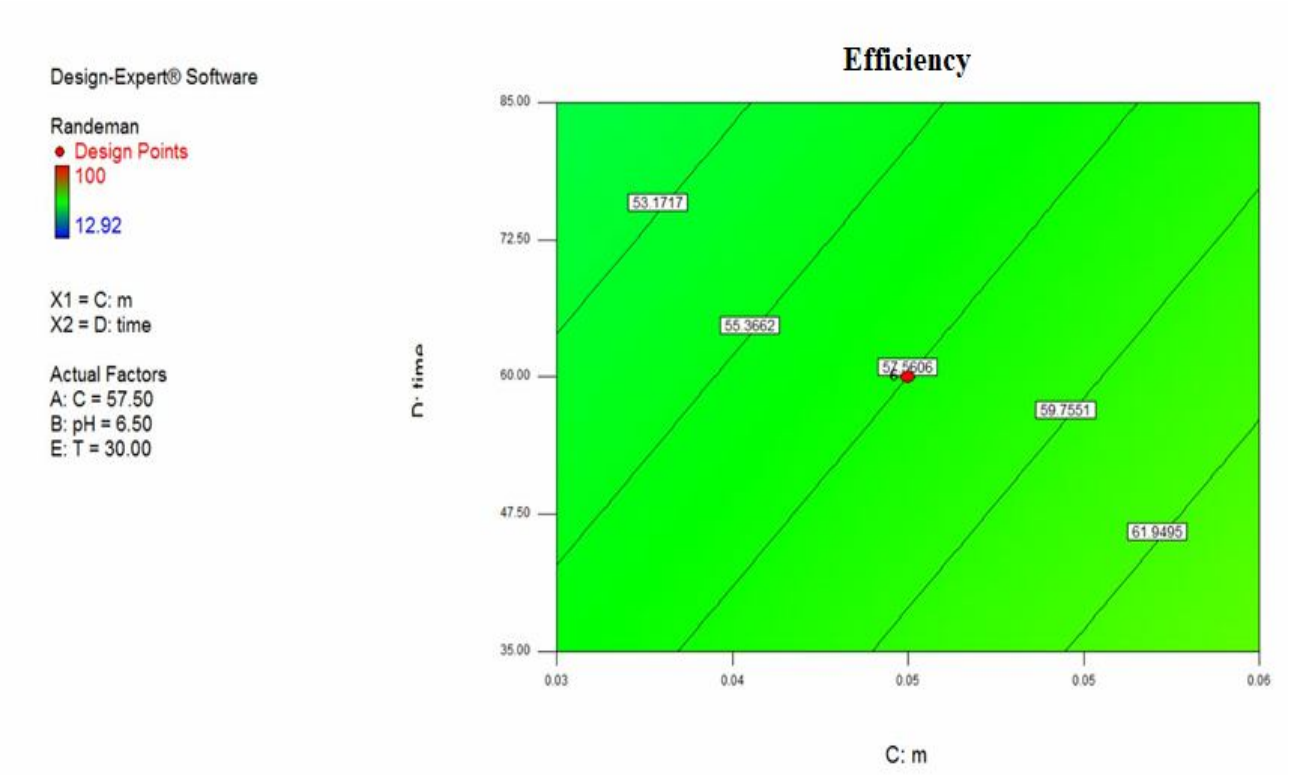

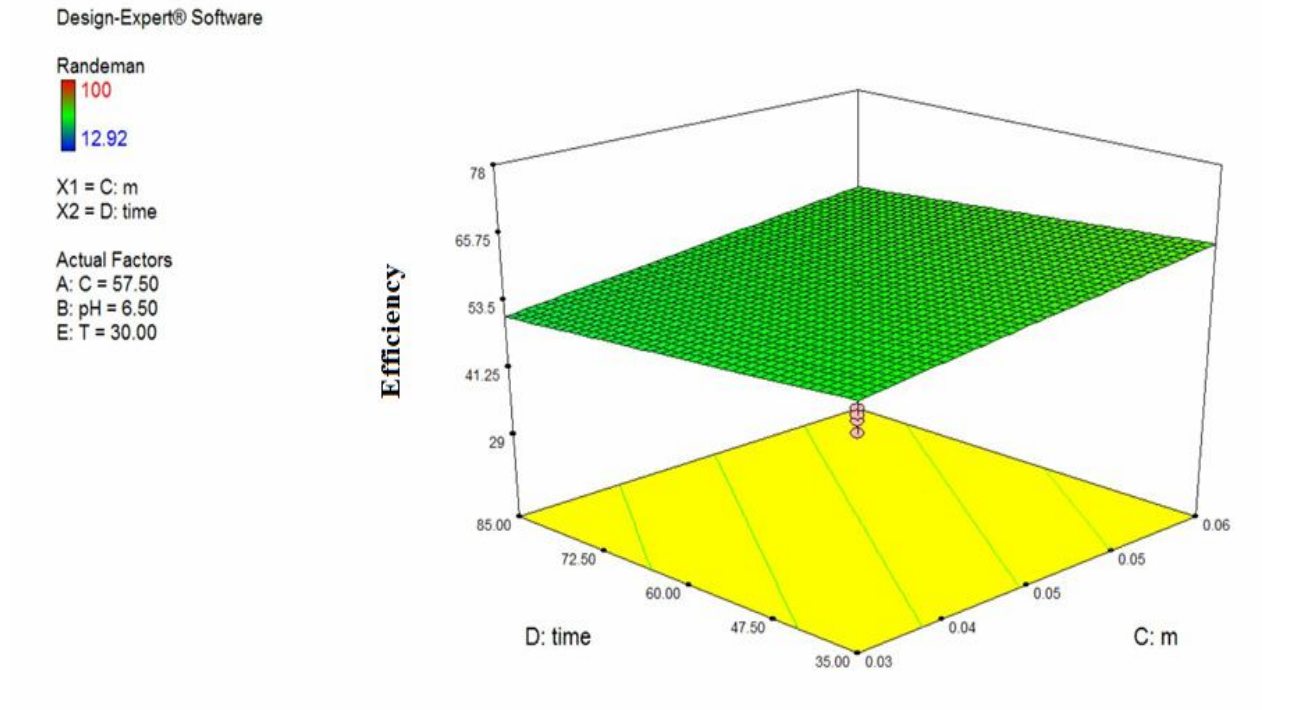

(c)

Fig. 5. Continued.

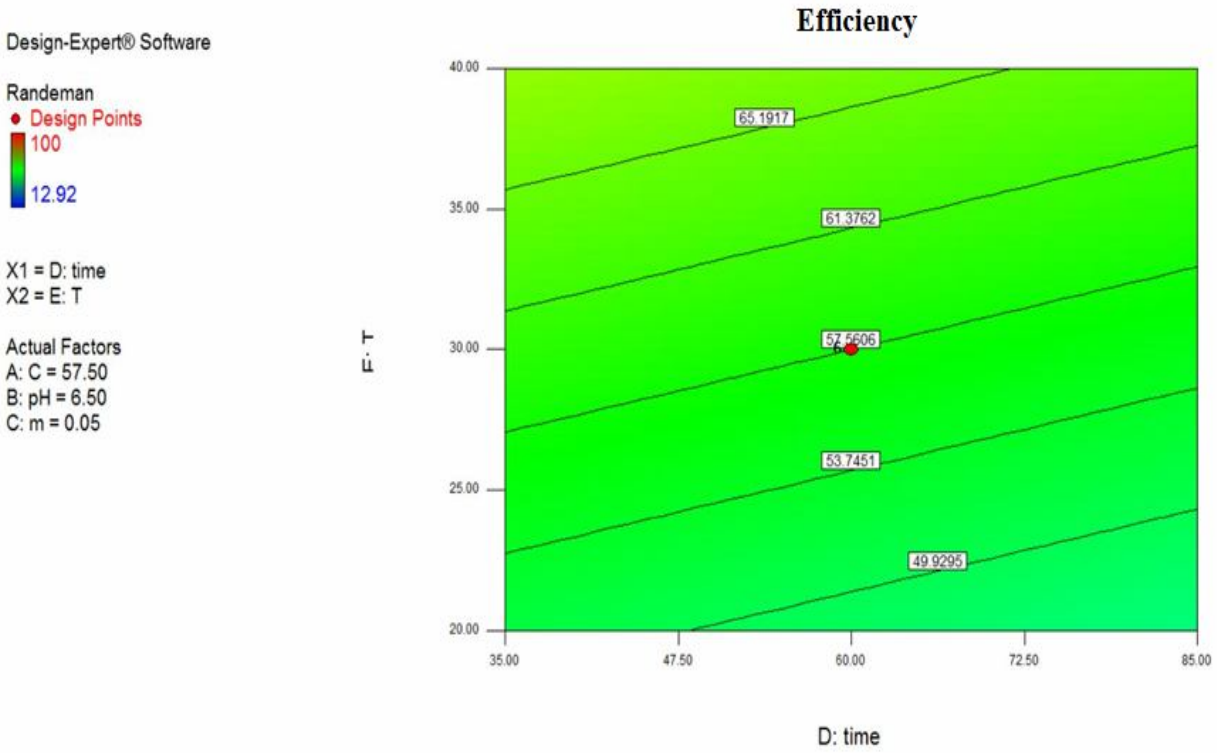

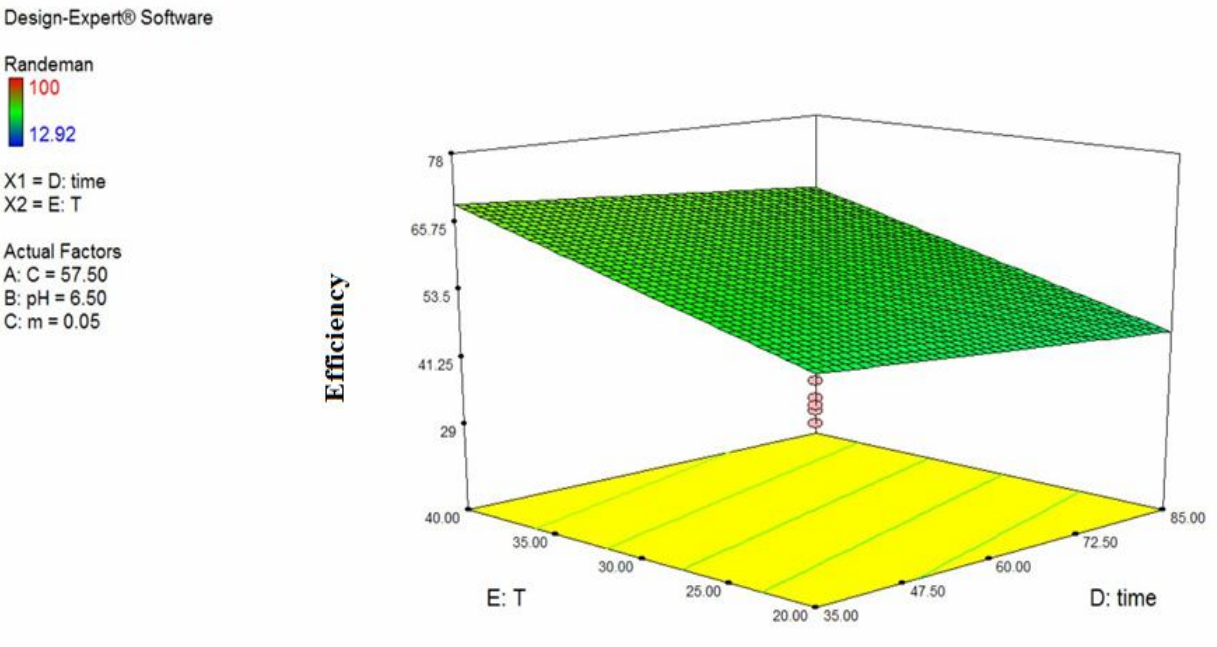

(d)

Fig. 5. Continued.

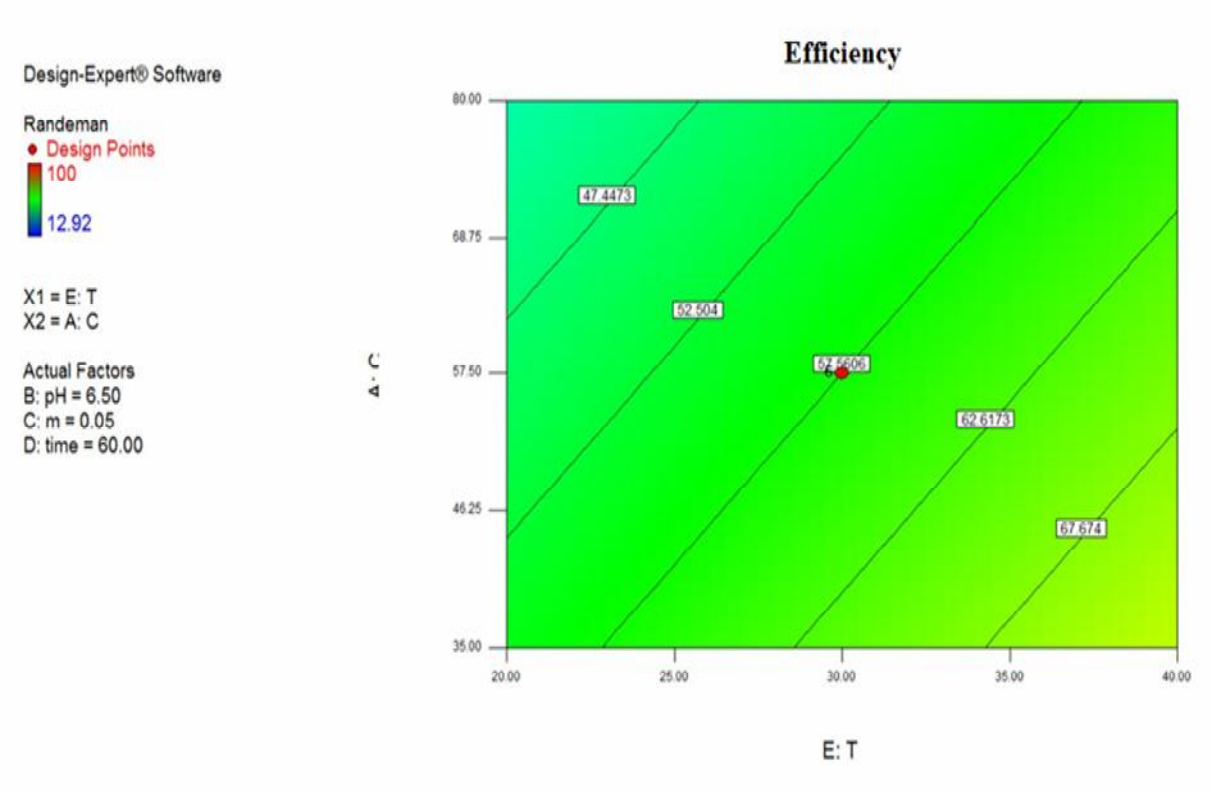

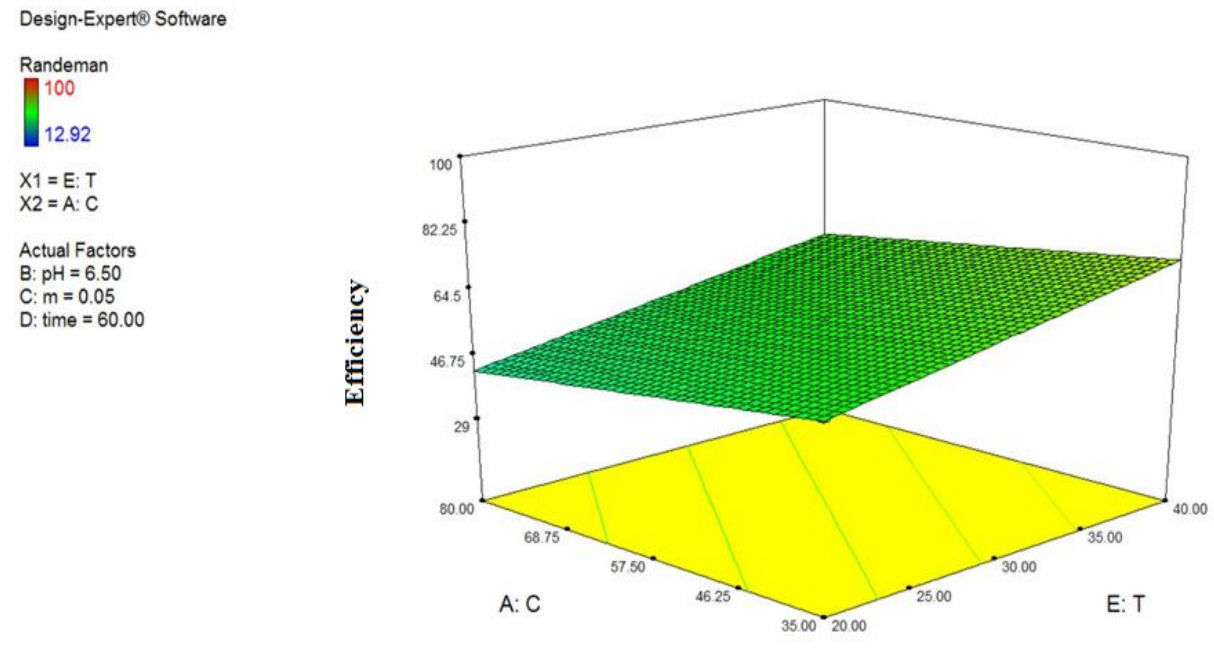

(e)

Fig. 5. Continued.

Table 4. The Results of ANOVA for the Response 1, %Efficiency, Surface Linear Model

Source	Sum of squares	df	Mean square	F Value	p-value Prob > F	
Model	8736.82	5	1747.36	3.63	0.0127	Significant
A-C	960.39	1	960.39	2.00	0.1696	
B-pH	5356.29	1	5356.29	11.13	0.0026	
C-m	380.33	1	380.33	0.79	0.3822	
D-time	162.55	1	162.55	0.34	0.5661	
E-T	1877.26	1	1877.26	3.90	0.0590	
Residual	12512.82	26	481.26			
Lack of fit	12476.89	21	594.14	82.66	< 0.0001	Significant
Pure error	35.94	5	7.19			
Cor total	21249.64	31				

df: degrees of freedom. SS: sums of squares, the sum of the squared differences between the average values and the overall mean. Ms: mean squarees, the sum of squares deviced by df. SD: standard deviation. R^2: R-Squared (coeffient of determination). F-value: test for comparing term variance with residual (error) variance. Prob > F: the probability of seeing the observed F value if the null hypothesis is true. Residual: consists of terms used to estimate the experimental error. Lack of fit: variation of the data arround the fitted model. Pure error: variation in the response in replicated design points. Cor total: totals of all information corrected for the mean.

Table 5. Optimization Point of Zn_2Al-LDH/Q

C*	pH*	m*	Time*	T*	Desirability	
35	4.17	0.03	51	32.5	1.000	Selected

of 54.89 implies that the model is significant and only 0.01% chance that a "model F value" this large could occur due to noise. The p-value of the model also is significant; $p < 0.0001$. The lack of fit is 3.63 and this is significant relative to the pure error when $p = 0.0127$. The insignificance of lack of fit value shows a good predictability. The "Pred R-Squared" of 0.1184 is in reasonable agreement with the "Adj R-Squared" of 0.2979 and shows a good predictability. Table 6 shows the chosen amounts for the equilibrium isotherms models , adsorption kinetics , and thermodynamic study in base of optimum condition.

Equilibrium Isotherms Models

Adsorption phenomena are typically shown through isotherms representing the amount of adsorbate on the

Table 6. Experimental Factors Used for Isotherm, Kinetic and Thermodynamic

Factors	Unit	Type of study	Levels						
Concentration (C)	mg l^{-1}	Isotherm	5	15	25	*35**	45	55	65
pH			4.17	4.17	4.17	*4.17**	4.17	4.17	4.17
Adsorbent dosage (m)	g l^{-1}		0.03	0.03	0.03	*0.03**	0.03	0.03	0.03
Contact time (time)	min	Kinetic	36	41	46	*51**	56	61	66
Temperature (T)	°C	Thermodynamic	17.5	22.5	27.5	*32.5**	37.5	42.5	47.5

Table 7. Isotherm Constant Parameters and Correlation Coefficients Calculated for the Adsorption of Cd^{2+} onto Zn_2Al-LDH/Q

Isotherms	Parameters	Value
Langmuir	q_m (mg g^{-1})	1.4424
	K_L (l mg^{-1})	-0.3550
	R^2	0.954
Freundlich	n	3.0845
	K_f (mg g^{-1}) (l $mg^{-1})^{1/n}$	1.2813
	R^2	0.8257
Temkin	B_t	1.7784
	K_T (l mg^{-1})	0.5569
	R^2	0.9153

adsorbent as a function of the adsorbate pressure (in case of gas) or concentration (in case of liquid) at a constant temperature. The equilibrium adsorption isotherm is used to give useful information about the mechanism, properties and tendency of adsorbent toward Cd^{2+}. In other words, adsorption isotherms represent extent and mechanism of process which is proportional to surface properties which simply estimate fitting experimental equilibrium data to different models such as Langmuir, Freundlich, and Tempkin. According to our previous reports [43], and based on their linear form, slopes and intercepts, respective constants are evaluated (Table 7). Also, experimental results based on the higher values of correlation coefficients ($R^2 \sim 1$) showed a reasonable applicability of Langmuir model for Cd^{2+} adsorption onto Zn_2Al-LDH/Q.

The experimental results from adsorption of Cd^{2+} by Zn_2Al-LDH/Q were analyzed by Langmuir, Freundlich and

Tempkin models. The Langmuir isotherm can be considered as Eq. (5) [43]:

$$C_e/q_e = 1/q_{\max} K_L + C_e/q_{\max} \quad (5)$$

where q_e (mg g^{-1}) and C_e (mg g^{-1}) are the amounts of adsorbed dye per unit mass of adsorbent and unadsorbed dye concentration in solution at equilibrium, respectively, q_{max} is the maximum amount of the Amaranth dye per unit mass of adsorbent on the surface bound at high C_e (mg g^{-1}), and K_L is adsorption equilibrium constant (l mg^{-1}). Figure 6a shows the linear plot of C_e/q_e *vs*. C_e of Langmuir isotherm. The values of q_{max} and K_L were determined from slope and intercepts of the plots and are presented in Table 7.

The Freundlich's adsorption isotherm model can be applied for a multilayer heterogeneous adsorption and expressed as Eq. (6) [44]:

$$\log q_e = 1/n \log C_e + \log K_F \quad (6)$$

where q constants are related to the maximum adsorption capacity and n is the intensity of adsorption. Figure 6b shows the linear plot of ($\log q_e$ *vs*. $\log C_e$) of Freundlich isotherm. The plot of $\log q_e$ *vs*. $\log C_e$ was employed to generate the intercept value of K_F and the slope of $1/n_F$ (Table 4). The heat of the adsorption and the interaction of adsorbent adsorbate were studied using Tempkin isotherm model as expressed in Eq. (7) [45]:

$$q_e = B_T \ln K_T + B_T \ln C_e \quad (7)$$

In this model, B_t is the Tempkim constant related to the heat of adsorption (J mol^{-1}), T is the absolute temperature (K), and K_T is the equilibrium binding constant (l mg^{-1}). Figure 6c shows the linear plot of q_e *vs*. $\ln C_e$ of Tempkim isotherm model. The constant parameters of isotherm equations and the correlation coefficient (R^2) for isotherm models are summarized in Table 5. The high correlation coefficient at various conditions shows the applicability of Tempkin model for investigation of the experimental data.

Adsorption Kinetics

Kinetic study can provide valuable insights into the reaction pathways and the mechanism of adsorption is a surface phenomenon resulting from the binding forces between atoms, molecules and ions of adsorbate and the surface of adsorbent [46,47]. In order to control the mechanisms of the adsorption processes such as mass transfer and chemical reactions, different kinetic models are used. The sorption reactions and also the rate of adsorption, as a factor in efficiency of adsorbent, and the mechanism of adsorption can be concluded from this studies. Adsorption kinetics of Cd^{2+} was evaluated using four models such as pseudo-first-order, pseudo-second order, intra particle diffusion, and Elovich models (39 Lin Deng).The various parameters were calculated from the plots of the kinetic model equations (Table 8). All the kinetic equations are shown in Table 8, where k_1 and k_2 (g mg^{-1} min^{-1}) are the pseudo-first-order and pseudo-second-order rate constants for adsorption. R^2 is the correlation coefficient to express the uniformity between the model-predicted values and the experimental data. α (mg g^{-1} min^{-2}) is the initial adsorption rate. β (g mg^{-1} min^{-1}) is the desorption constant related to the extent of surface coverage and activation energy for chemisorption. All of the investigated models were fitted by a linear regression to the experimental data, evaluating their appropriateness based on the corresponding correlation coefficients R^2. The correlation coefficient (R^2) and agreement between the experimental and calculated values of q_e are the criteria for applicability of each model. Good agreement between two q_e values and the high values of ($R^2 \sim 1$) indicate that the adsorption system under study follows the pseudo-first order kinetic model (Table 8). A pseudo-first order adsorption mechanism assumes the rate of occupying adsorption sites is proportional to the square of the number of unoccupied sites.

Table 8 summarizes the obtained results of each model. The highest R^2 value of this model (1.0000) confirm the applicability of this model to interpret the experimental data. From all the correlation coefficients and above analysis, it can be concluded that the pseudo-first-order kinetic model is the most suitable model for adsorption of Cd^{2+} onto Zn_2Al-LDH/Q, indicating that the adsorption process is mainly controlled by chemical adsorption and ion exchange and surface adsorption mechanism occur in the

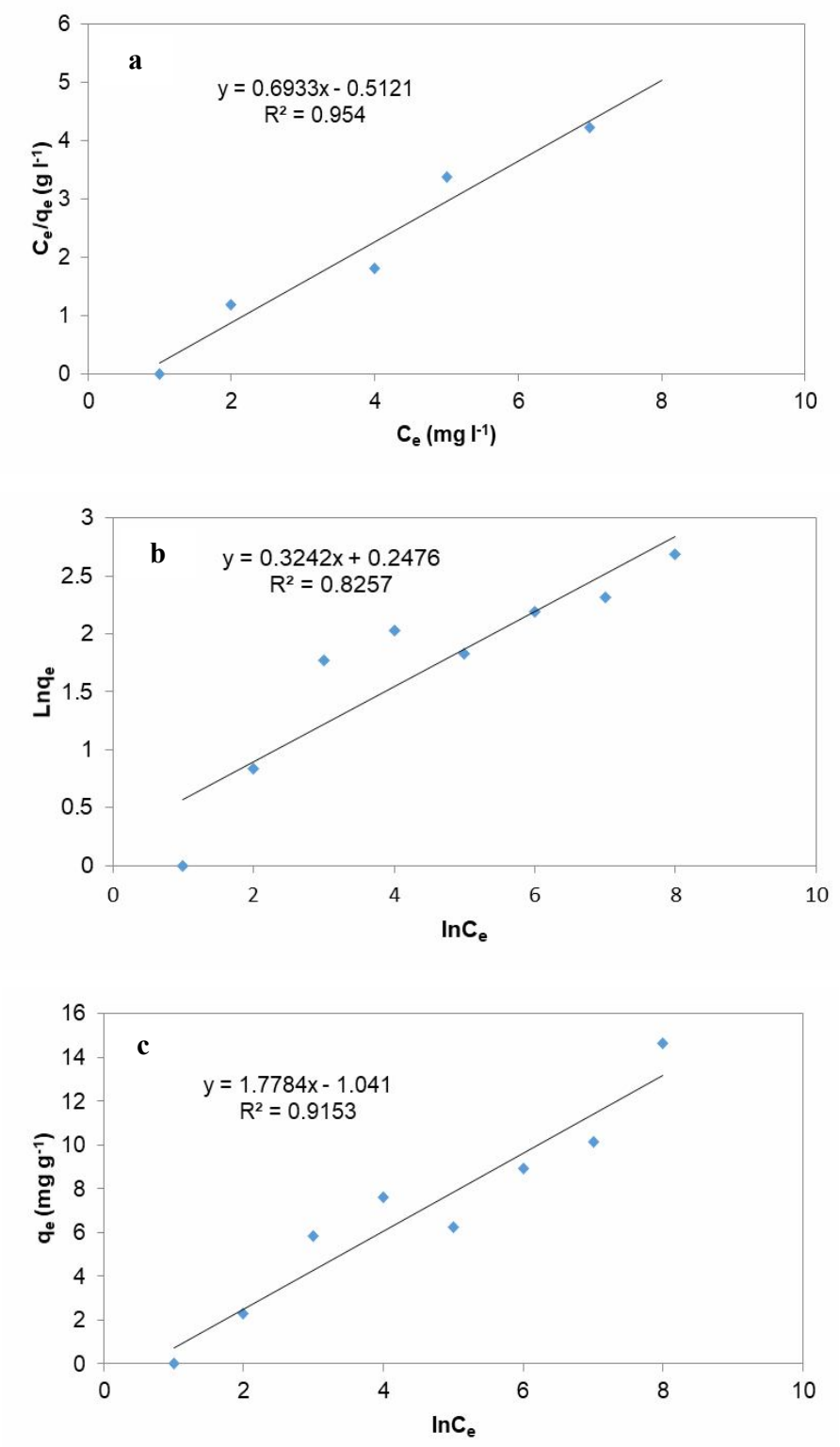

Fig. 6. The plots of (a) Langmuir equilibrium isotherm, (b) Frundlich isotherm, and (c) Tempkin isotherm.

Table 8. Kinetic Parameters for Removal of Cd^{2+} onto Zn_2Al-LDH/Q

Model	Equation	Parameters	Value
Pseudo-first-order	$\log(q_e - q_t) = \log(q_e) - \frac{k_1 t}{2.303}$	K_1 (min^{-1})	-0.0492
		q_e	16.8172
		R^2	0.9686
Pseudo-second-order	$\frac{t}{q_t} = \frac{1}{k_2 q_e^2} + \left(\frac{1}{q_e}\right)t$	k_2 (g mg^{-1} min^{-1})	1154.033
		qe	-9.7752
		R^2	0.915
		K_{id}	0.8066
Intraparticle diffusion	$q_t = K_{id} t^{1/2} + C$	C	6.12
		R^2	0.146
Elovich	$q_t = 1/\beta \ln(\alpha\beta) + 1/\beta \ln(t)$	α	0.45376
		β	0.3516
		R^2	0.1474

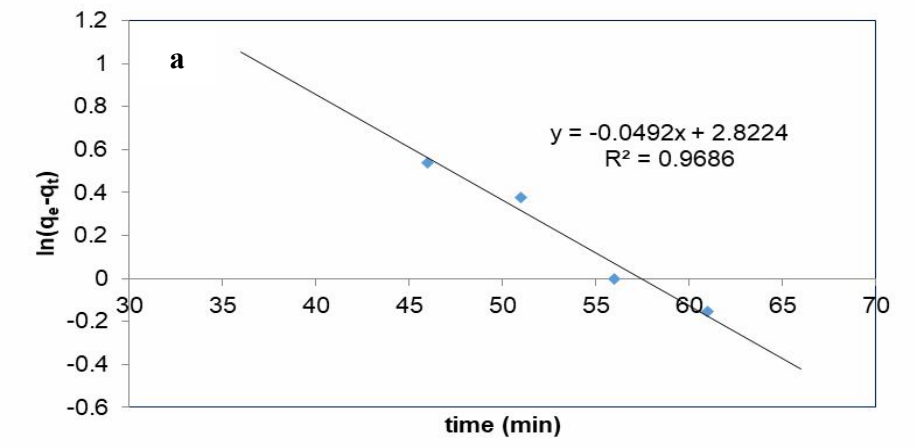

Fig. 7. The plots of (a) pseudo- first- order, (b) pseudo-second-order and (c) intra particle diffusion (d) Elovich.

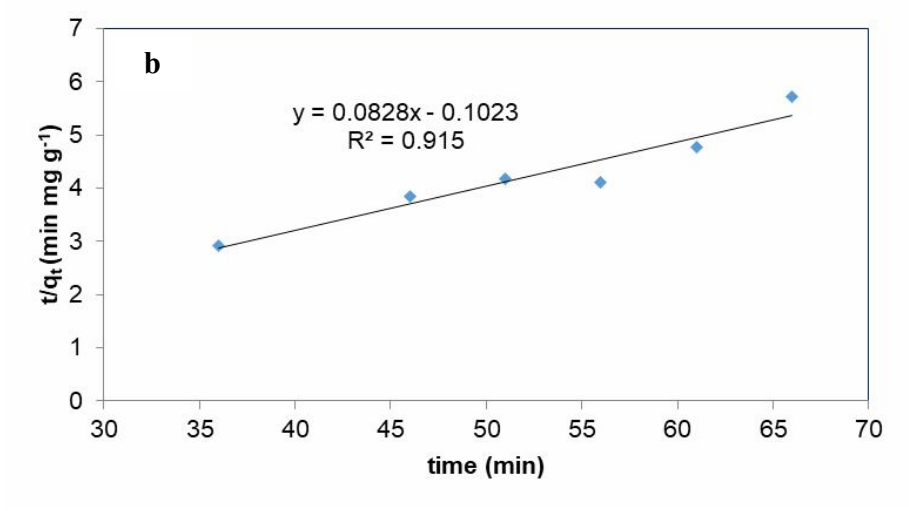

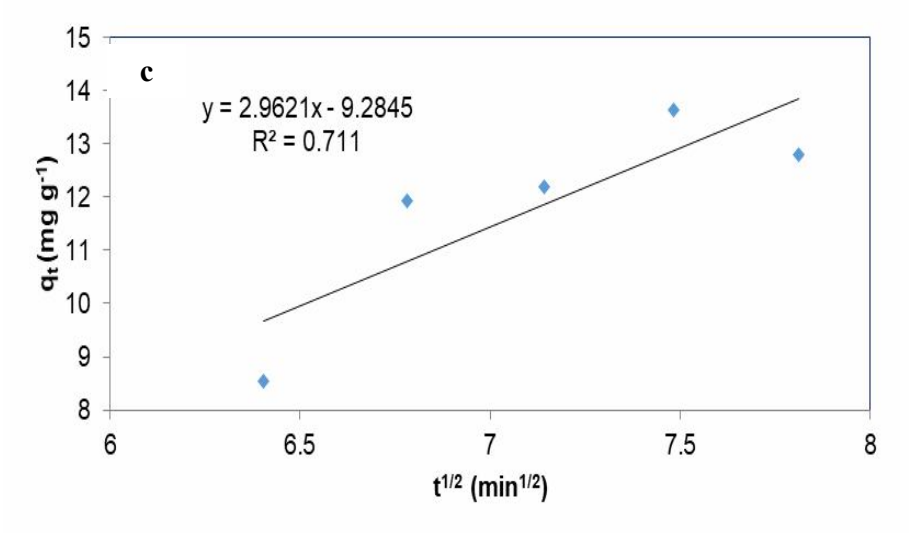

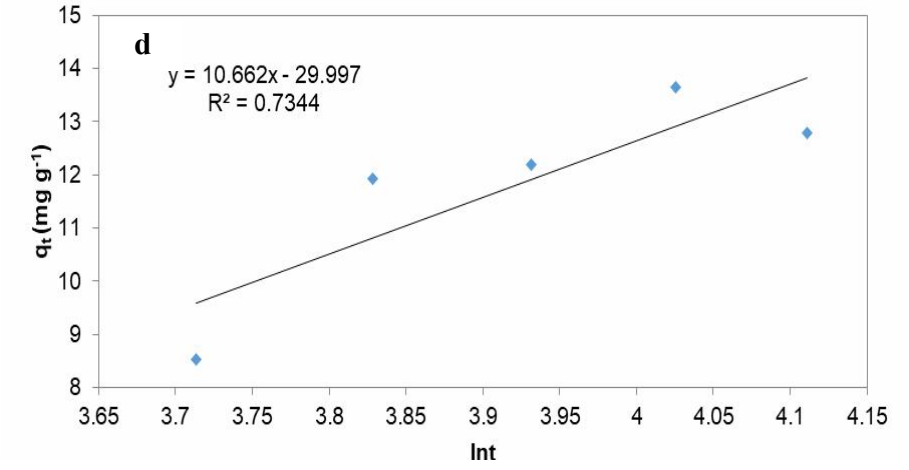

Fig. 7. Continued.

adsorption process. Based on the correlation coefficients and analysis performed, it can be concluded that the pseudo-first-order kinetic model is the most suitable model for adsorption of Cd^{2+} onto Zn_2Al-LDH/Q, indicating that the adsorption process is mainly controlled by chemical adsorption and ion exchange, and that surface adsorption mechanism occurs in the adsorption process.
The equation of this model is Eq. (8):

$$\ln(q_e - q_t) = \ln q_e - K_1 t \tag{8}$$

where q_e is the equilibrium adsorption capacity (mg g^{-1}) for the pseudo-first-order of the adsorption, q_t is the adsorption capacity at time t (mg g^{-1}) and k_1 (min^{-1}) is the rate constant of the pseudo-first-order adsorption. The values of q_e and k_1 are obtained from the slope and intercept of $\ln(q_e - q_t)$ *vs.* t. According to the assumptions of this model, adsorption process involves different mechanisms including chemical and electrostatic interactions between functional groups on the surface of adsorbent and adsorbate molecules .The linear regressions and kinetic parameters are listed in Fig. 7 and Table 8, respectively.

It is clear that correlation coefficients for the pseudo-first-order model ($R^2 \sim 0.97$) are higher than that for the pseudo-second-order model ($R^2 = 0.915$), indicating that the present system can be well defined by the pseudo-first-order kinetic model in the adsorption step. Additionally, the theoretical equilibrium sorption capacity ($q_{e,cal}$) calculated by the pseudo-first-order model at all concentrations are also in good agreement with those obtained from experiments ($q_{e,exp}$). The fitness of the pseudo-first-order kinetic model reveals that the rate-limiting step in adsorption is controlled by chemical process [48]. The Elovich equation is the integration of the rate equation with the same boundary conditions as the pseudo-first-order equation, which is used to interpret the predominantly chemical adsorption on highly heterogeneous adsorbents [49]. As depicted in Fig. 7d, the plots of q_t *vs.* ln(t) display a relative good linear correlation, suggesting that the Elovich equation is able to describe the adsorption kinetic and ion exchange processes involved in the system. Due to the mesoporous structure of the adsorbent, diffusion is also expected to influence the adsorption rate. The plots of q_t *vs.* $t^{1/2}$ at different initial Cd^{2+} concentrations are illustrated in Fig. 7c. As observed, all the three plots exhibit multi-straight-line nature, indicating that more than one process affects the adsorption. The first rapid stage is attributed to mass transfer across the external boundary layer film to the outer surface of adsorbent particles (film diffusion) [50], the second linear portion refers to the pore diffusion that Cd^{2+} moves within the micro-, meso- and macro-pores of adsorbent particles (pore diffusion), and the third stage with the lowest slope is ascribed to the surface diffusion mechanism at a site on the adsorbent surface (physical/chemical reaction or surface diffusion) [50]. The fitting results imply that the intra-particle diffusion of Cd^{2+} to an adsorption site on the particle surface is the rate limiting step in the adsorption process. All the intra-particle diffusion rate constants C related to the boundary layer thickness in this study are not zero, revealing that the adsorption process may not be mainly controlled by intra-particle diffusion [51]. The kinetic analysis based on the kinetic models including pseudo first- and second-order, Elovich and intraparticle diffusion (Figs. 7a-d) provides valuable information about the rate and mechanism of adsorption.

Thermodynamic Study

Thermodynamic consideration of an adsorption is dispensable to deduce whether the process takes place spontaneously or not, and provides in-depth information about internal energy changes that are associated with. The change in thermodynamic parameters such as Gibbs free energy (ΔG°), enthalpy change (ΔH°), and entropy change (ΔS°) for the adsorption system are obtained using the following equations [48]:

$$\Delta G^\circ = -RT \ln K_C \tag{9}$$

$$\ln K_C = \frac{\Delta S^\circ}{R} - \frac{\Delta H^\circ}{RT} \tag{10}$$

where K_c (ml g^{-1}) is the solid-liquid distribution coefficient that can be obtained by the intercept of plot of $\ln(q_e/C_e)$ *vs.* q_e, R is the universal gas constant (8.314 J mol^{-1} K^{-1}) and T

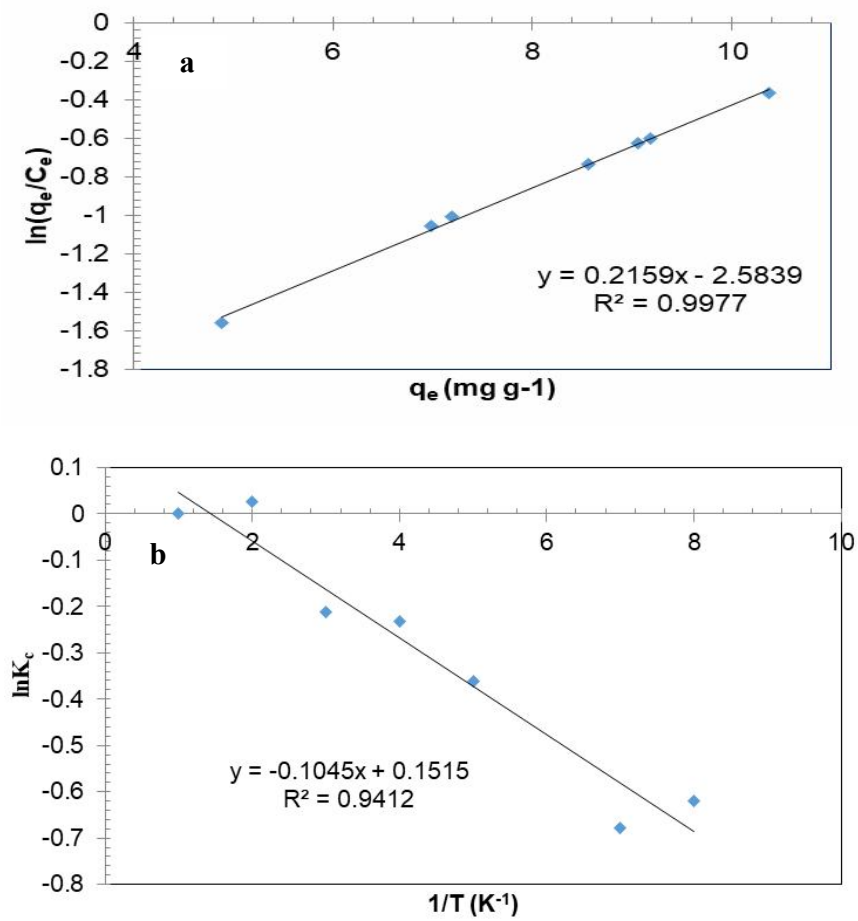

Fig. 8. The Vant Hoff plots of Zn_2Al-LDH/Q adsorption to determine (a) ΔG°, (b) ΔH° and ΔS°.

Table 9. Values of Thermodynamic Parameters for Cd^{2+} with Zn_2Al-LDH/Q

Parameters	ΔH° (J mol^{-1})	ΔS° (J mol^{-1} K^{-1})	ΔG° (J mol^{-1})	lnK_C	R^2
Zn_2Al-LDH/Q	-0.8688	1.2596	-387.6567	0.1512	0.9412

is the absolute temperature. The plots of lnK_c *vs.* 1/T give the straight line from which ΔH° and ΔS° are calculated from the slope and intercept, respectively (Fig. 8).

The positive value of ΔH° (-0.8688 J mol^{-1}) suggests that the adsorption process is exothermic. The negative value of ΔS° (1.2596 J mol^{-1} K^{-1}) also suggests a decreased random at the solid-solution interface during the fixation of Cd^{2+} on the active sites of the adsorbent.

Reusability of the Zn_2Al-LDH/Q

The ability of reusing the adsorbents in several successive separation processes was examined. The obtained results showed that Zn_2Al-LDH/Q can be reused for five times without any decrease in their efficiency

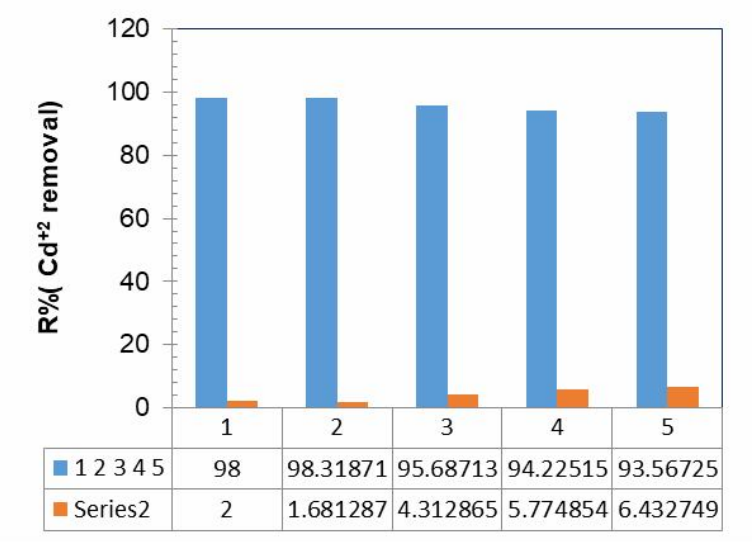

Fig. 9. The ability of reusing Zn_2Al-LDH/Q in five successive separation processes.

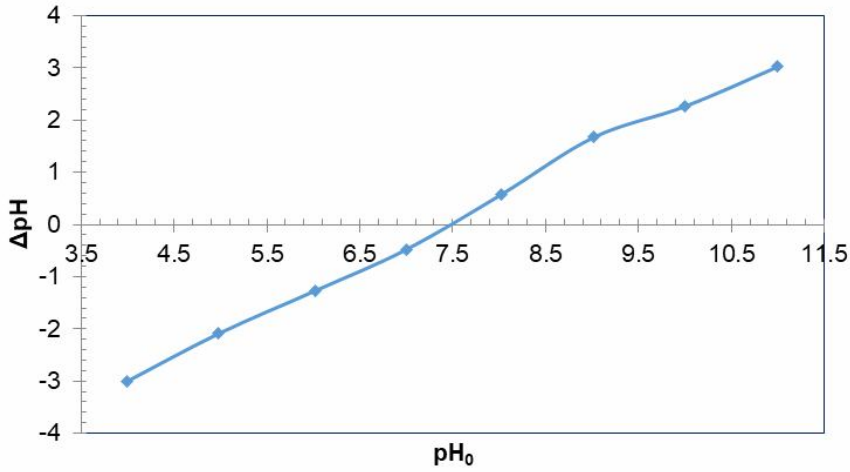

Fig. 10. Zero point charge determination.

(Fig. 9).

Determination of Zero point Charge

Determination of point of zero charge (pHz) was done to determine the surface charge (or the stability) of Zn_2Al-LDH/Q. For the determination of pHz, 0.1 M NaCl was prepared, and its initial pH was adjusted between 4.0 and 11.0 using HCl and NaOH. Then, 20 ml of 0.1 M NaCl was taken in 25 ml flasks and 0.036 g of Zn_2Al-LDH/Q was added to each solution. These flasks were kept for 24 h and the final pH of the solutions was measured with a pH meter. Graphs were plotted between final pH and initial pH. From Fig. 10, it is clear that at 7.41, ΔpH = 0, therefore, pHz = 7.41.

The adsorption studies for Cd^{2+} was carried out at pH 7.4 based on the zeta potential analysis of the Zn_2Al-LDH/Q adsorbent which has been previously discussed. Thus, the adsorption of the ions such as Pb^{2+},

Table 10. Comparison of Adsorption Capacities of Various Adsorbents for the Removal of Cd^{2+} from Aqueous Solution

Adsorbent	q_{max} (mg g^{-1})	Ref.
FeMnMg-LDH	59.99	
Nano hydroxyapatite	9.8	[55]
NH_2-MCM-41	18.25	[56]
MgAl-Humate-LDH	39.2	[57]
MgAl-Cl-LDH	71.15	[58]
MgAl-H100-LDH	53.95	
MgAl-H50-LDH	27.79	
MgAl-edta-LDH	17	[59]
MgAl-CO_3-LDH	1	
ZnAl-DTPA-LDH	44.8	[60]
ZnAl-DSMA-LDH	112	
ZnAl-NO_3-LDH	3.02	
ZnAl-edta-LDH	42.15	[61]
MgAl-CO_3-LDH	61.4	[62]
Fe_3O_4/MgAl-CO_3-LDH	45.6	
Clinoptilolite	4.88	[63]
Tourmaline	33.11	[64]
Zn_2Al-LDH/Q	1.44	This work

Table 11. Application of Zn_2Al-LDH/Q for Removal of Cd^{2+} in Real Sample

Run	Wast water (cc)	Concentration of Cd^{2+} (mg l^{-1})	pH	Adsorbent (g)	T (°C)	Time (min)	%R	q_e (mg g^{-1})
1	50	0	4.17	0.03	35.2	51	14.4201	0.188968
2	50	1	4.17	0.03	35.2	51	7.22311	0.146440678
3	50	2	4.17	0.03	35.2	51	9.77528	0.336537162
4	50	3	4.17	0.03	35.2	51	9.0035	0.427740864
5	50	4	4.17	0.03	35.2	51	6.55080	0.350118243
6	50	5	4.17	0.03	35.2	51	6.97143	0.472231293

Table 12. Application of Zn_2Al-LDH/Q for Investigation of Interfering of other Heavy Metal Ions in a Real Sample

Run	Element	C ($mg\ l^{-1}$)	Run	Element	C ($mg\ l^{-1}$)
1	As	0.009	14	Co	0.08
2	Cd	1.97	15	Li	0.11
3	Se	0.09	16	Mn	1.25
4	Pb	3.56	17	Ti	0.21
5	Cr	7.06	18	Zn	1.44
6	Fe	48.1	19	Bi	<0.1
7	Mo	0.39	20	Sr	20.8
8	Sn	2.82	21	Ni	5.59
9	Sb	0.25	22	W	<0.1
10	Al	4.58	23	Pd	<0.002
11	V	0.03	24	Na	843
12	Ba	0.05	25	Si	0.58
13	Cu	0.51	26	K	67.4

Table 13. Application of Zn_2Al-LDH/Q for Removal of Cd^{2+} in a Real Sample after Adsorption

Run	Wast water (cc)	Concentration of Cd^{2+} ($mg\ l^{-1}$)	pH	Adsorbent (g)	T (°C)	Time (min)	%R	q_e ($mg\ g^{-1}$)	%Recovery
1	50	0	4.17	0.03	35.2	51	14.4201	0.1889	-
2	50	1	4.17	0.03	35.2	51	7.2231	0.1464	152
3	50	2	4.17	0.03	35.2	51	9.7753	0.3365	142.75
4	50	3	4.17	0.03	35.2	51	9.0035	0.4277	137.5
5	50	4	4.17	0.03	35.2	51	6.5508	0.3501	147.125
6	50	5	4.17	0.03	35.2	51	6.9714	0.4722	143.1

Cd^{2+}ions in the adsorbate may be due to the interaction of the species that are dominant at pH < 8, such as Pb^{2+}, Cd^{2+}, $Pb(OH)^{+}$ and $Cd(OH)^{+}$ with the functional groups on the adsorbent surface (active hydroxyl groups on the Zn_2Al-LDH materials) [52]. So, metal ions that can interact with the functional groups on the adsorbent improves the probability of metal ion removal. Thus, due to the multiple-ion-binding sites on the adsorbent surfaces and the metal ion species a number of metal adsorbent complexes are formed during sorption process [53,54].

A comparison of the Cd^{2+} removal efficiency between the Zn_2Al-LDH/Q in this study and other sorbents reported in literature is given in Table 10. The results showed that Zn_2Al-LDH/Q in this work has a high adsorption capacity making it appropriate to be used as potential efficient adsorbent for the heavy metal removal from aqueous solutions.

Application of Zn_2Al-LDH/Q in a Real Sample

To evaluate the applicability of the optimized adsorption method, the synthesized adsorbent Zn_2Al-LDH/Q was used for the removal of Cd^{2+} from seawater collected from Battery factories as a real sample. Table 11 shows the experimental conditions and the obtained analytical results as well as the percentage removal e-ciencies and adsorption capacity.

Also, in order to show the effects of interfering of other heavy metal ions with the action of Zn_2Al-LDH/Q in adsorbing Cd^{+2}, we performed more experiments on the real sample. The elements in Table 12 were found in the battery unit wastewater sample reported by the ICP analysis. Tables 12 and 13 show the analytical results before adsorption and after adsorption as well as the percentage removal e-ciencies.

In the presence of these cationic disturbances as well as severe anionic sulfate disturbance in the effluent, Cd^{2+} adsorption was carried out and the results showed an increase in the amount of Cd^{2+} ions from 137.5-152%, and through correction and based on the recovery, the adsorption values were applied to estimate the values of qe and %R.

CONCLUSIONS

This study indicates the Zn_2Al-LDH/Q potential as an efficient adsorbent for removal of Cd(II) from wastewater. CCD was employed to rate the effects of parameters on the removal efficiency of Cd(II) ions. The optimum conditions for maximum Cd(II) adsorption were initial Cd^{2+} concentration of 35 mg l^{-1}, a pH value of 4.17, adsorbent dosage of 0.03 g l^{-1}, the temperature of 32.5 °C, and contact time of 51 min. In optimum conditions, the amount adsorbed and the maximum removal yield were calculated to be 12.18 mg g^{-1} and 45%, respectively. The results obtained for the adsorption of Cd(II) ions from aqueous solutions were tested with some isotherm equations and it was determined that Langmuir isotherm is more compatible than the others are. Moreover, the kinetic data fitted very well with the pseudo-first-order model. Thermodynamic studies showed that the adsorption process was spontaneous and exothermic. As a result, Zn_2Al-LDH/Q can be chosen as an effective adsorbent for treating heavy metals from wastewater.

ACKNOWLEDGEMENTS

The financial support of the research council of Payame Noor University of Isfahan is gratefully acknowledged.

REFERENCES

[1] Farasati, M.; Haghighi, S.; Boroun, S., Cd removal from aqueous solution using agricultural wastes. *Desalin. Water Treat.* **2016**, *57*, 11162-11172, DOI: org/10.1080/19443994.2015.1043588.

[2] Sheng, J.; Qiu, W.; Xu, B.; Xu, H.; Tang, C., Monitoring of heavy metal levels in the major rivers and in residents blood in Zhenjiang City, China, and assessment of heavy metal elimination via urine and sweat in humans. *Environ. Sci. Pollut. Res.* **2016**, *23*, 11034-11045, DOI: org/10.1007/s11356-016-6287-z.

[3] Dey, P.; Gola, D.; Mishra, A.; Malik, A.; Singh, D. K.; Patel, N.; Von Bergen, M.; Jehmlich, N., Comparative performance evaluation of multi-metal resistant fungal strains for simultaneous removal of multiple hazardous metals. *J. Hazard. Mater.* **2016**, *318*, 679-685, DOI: org/10.1016/ j.jhazmat.2016.07.025.

[4] WHO, "Guidelines for the Safe Use of Wastewater,

Excreta and Greywater", World Health Organization. 2006, Vol. I, p. 95.

[5] Nordberg, G. F.; Nogawa, K.; Nordberg, M., Cadmium, Handbook on the Toxicology of Metals, fourth edition, 2014, p. 667-716.

[6] Mohammadnezhad, G.; Dinari, M.; Soltani, R., The preparation of modified Boehmite/PMMA nanocomposites by in situ polymerization and the assessment of their capability for Cu^{2+} ion removal. *New J. Chem.* **2016**, *40*, 3612-3621, DOI: 10.1039/C5NJ03109E.

[7] Cui, H.; Fan, Y.; Yang, J.; Xu, L.; Zhou, J.; Zhu, Z., In situ phytoextraction of copper and cadmium and its biological impacts in acidic soil. *Chemosphere.* **2016**, *161*, 233-241, DOI: org/10.1016/ j.chemosphere.2016.07.022.

[8] Dinari, M.; Soltani, R.; Mohammadnezhad, G., Kinetics and thermodynamic study on novel modified-mesoporous silica MCM-41/polymer matrix nanocomposites: effective adsorbents for trace Cr(VI) removal. *J. Chem. Eng. Data*. **2017**, *62*, 2316-2329, DOI: org/10.1021/acs.jced.7b00197.

[9] Lee, C. G.; Park, J. A.; Choi, J. W. ; Ko, S. O.; Lee, S. H., Removal and recovery of Cr(VI) from industrial plating wastewater using fibrous anion exchanger. *Water Air Soil Pollut.* 227, **2016**, 456, DOI: org/10.1007/s11270-016-3147-x.

[10] Li, M.; Gong, Y.; Lyu, A.; Liu, Y.; Zhang, H., The applications of populous fiber in removal of Cr(VI) from aqueous solution. *Appl. Surf. Sci.* **2016**, *383*, 133-141, DOI: .org/10.1016/j.apsusc.2016.04.167

[11] Mohammadnezhad, G.; Abad, S.; Soltani, R.; Dinari, M., Study on thermal, mechanical and adsorption properties of amine-functionalized MCM-41/PMMA and MCM-41/PMMA nanocomposites prepared by ultrasonic irradiation. *Ultrason. Sonochem.* **2017**, *39*, 765-773, DOI: 10.1016/j.ultsonch.2017.06.001.

[12] Visa, M.; Chelaru, A. M., Hydrothermally modified fly ash for heavy metals and dyes removal in advanced wastewater treatment. *Appl. Surf. Sci.* **2014**, *303*, 14-22, DOI: org/10.1016/j.apsusc.2014.02.025.

[13] Yang, K.; Yan, L. G.; Yang, Y. M.; Yu, S. J.; Shan, R. R.; Yu, H. Q.; Zhu, B. C.; Du, B., Adsorptive removal of phosphate by Mg-Al and Zn-Al layered double hydroxides: kinetics, isotherms and mechanisms. *Sep. Purif. Technol.* **2014**, *124*, 36-42, DOI: org/10.1016/ j.seppur. 2013.12.042.

[14] Ahmadi, F; Esmaeili, H., Chemically modified bentonite/Fe_3O_4 nanocomposite for Pb(II), Cd(II), and Ni(II) removal from synthetic wastewater. *Desalin Water Treat.* **2018**, *110*, 154-167, DOI: 10.5004/dwt.2018.22228.

[15] Foroutan, R.; Mohammadi, R.; Farjadfard, S.; Esmaeili, H.; Saberi, M.; Sahebi, S.; Dobaradaran, S.; Ramavandi, B., Characteristics and performance of Cd, Ni, and Pb bio-adsorption using Callinectes sapidus biomass: real wastewater treatment. *Environ Sci Pollut Res Int.* **2019**, *26*, 6336-6347, DOI: org/10.1007/s11356-018-04108-8.

[16] Khoshkerdar, I.; Esmaeili, H., Adsorption of Cr(III) and Cd(II) Ions using Mesoporous Cobalt-Ferrite Nanocomposite from Synthetic Wastewater. *Acta Chimica Slovenica.* **2019**, *66*, 208-216, DOI: org/10.17344/acsi.2018.4795.

[17] Foroutana, F.; Esmaeilib, H.; Sanatic, A. M.; Ahmadid, M.; Ramavandif, B., Adsorptive removal of Pb(II), Ni(II) and Cd(II) from aqueous media and leather wastewater using Padinasanctae-crucis biomass. *Desalin Water Treat.* **2018**, *135*, 236-246, DOI: 10.5004/dwt.2018.23179.

[18] Das, J.; Das, D.; Parida, K. M., Preparation and characterization of Mg-Al hydrotalcite-like compounds containing cerium. *J. Colloid Interface Sci.* **2006**, *301*, 569-574, DOI: org/10.1016/ j.jcis.2006.05.014.

[19] Cai, X.; Shen, X.; Ma, L.; Ji, Z.; Xu, C.; Yuan, A., Solvothermal synthesis of NiCo-layered double hydroxide nanosheets decorated on RGO sheets for high performance supercapacitor. *Chem. Eng. J.* **2015**, *268*, 251-259, DOI: org/10.1016/j.cej.2015.01.072.

[20] Nishimura, Sh.; Takagaki, A.; Ebitani, K., Characterization, synthesis and catalysis of hydrotalcite-related materials for highly efficient materials transformations, *Green Chem.,* **2013**,*15*, 2026-2042, DOI:org/10.1039/C3GC40405F.

[21] Li, C.; Wei, M.; Evans, D. G.; Duan, X., Layered double hydroxide based nano materials as highly

efficient catalysts and adsorbents. *Small.* **2014**, *10*, 4469-4486, DOI: 10.1002/smll.201401464.

[22] Ladewig, K.; Xu, Z. P.; Lu, G. Q., Layered double hydroxide nanoparticles in gene and drug delivery. *Exp. Opin. Drug. Deliv.* **2009**, *6*, 907-922, DOI: 10.1517/17425240903130585.

[23] Kim, M. H.; Park, D. H.; Yang, J. H.; Choy, Y. B.; Choy, J. H., Drug inorganic-polymer nano- hybrid for transdermal delivery. *Int. J. Pharm.* **2013**, *444*, 120-127, DOI: 10.1016/j.ijpharm.2012.12.043.

[24] Das, J.; Patra, B. S.; Baliarsingh, N.; Parida, K. M., Adsorption of phosphate by layered double hydroxides in aqueous solutions. *Appl. Clay. Sci.* **2006**, *32*, 252-260, DOI: org/10.1016/ j.clay.2006.02.005.

[25] Goh, K. H.; Lim, T. T.; Dong, Z., Application of layered double hydroxides for removal of oxyanions: a review. *Water. Res.* **2008**, *42* 1343-1368, DOI: org/10.1016/j.watres.2007.10.043.

[26] Bharali, D.; Deka, R. C., Preferential adsorption of various anionic and cationic dyes from aqueous solution over ternary CuMgAl layered double hydroxide. *Colloids Surf. A* **2017**, *525*, 64-76, DOI:.org/10.1016j.colsurfa.2017.04.060.

[27] Abdellaoui, K.; Pavlovic, I.; Bouhent, M.; Benhamou, A.; Barriga, C., A comparative study of the amaranth azo dye adsorption/desorption from aqueous solutions by layered double hydroxides. *Appl. Clay. Sci.* **2017**, *143*, 142-150, DOI: org/ 10.1016/j.clay.2017.03.019.

[28] Dos Santos, R. M.; Gonçalves, R. G.; Constantino, V. R.; Santilli, C. V.; Borges, P. D.; Tronto, J.; Pinto, F. G., Adsorption of acid yellow 42 dye on calcined layered double hydroxide: e-ect of time, concentration, pH and temperature. *Appl. Clay. Sci.* **2017**, *140*, 132-139, DOI: 10.1016/j.clay.2017.02.005.

[29] Yao, W.; Yu, S.; Wang, J.; Zou,Y.; Lu, S.; Ai, Y.; Alharbi, N. S.; Alsaedi, A.; Hayat, T.; Wang, X., Enhanced removal of methyl orange on calcined glycerol-modifed nanocrystallined Mg/Al layered double hydroxides. *Chem. Eng. J.* **2017**, *307*, 476-486, DOI:org/10.1016/j.cej.2016.08.117.

[30] Becker, C. M.; Gabbardo, A. D.; Wypych, F.; Amico, S. C., Mechanical and flame-retardant properties of epoxy/Mg-Al LDH composites. Compos *Part A Appl. Sci. Manuf.* **2011**, *42*, 196-202, DOI: org/10.1016/ j.compositesa.2010.11.005.

[31] Gu, Z.; Atherton, J. J.; Xu, Z. P., Hierarchical layered double hydroxide nanocomposites: structure, synthesis and applications. *Chem. Commun.* **2015**, *51*, 3024-3036, DOI: 10.1039/b000000x.

[32] Carretero, M. I., Clay minerals and their benefcial e-ects upon human health. A review. *Appl. Clay. Sci.* **2002**, *21*, 155-263, DOI:org/10.1016/S0169-1317 (01)00085-0.

[33] Ahmed, I. M.; Gasser, M. S., Adsorption study of anionic reactive dye from aqueous solution to Mg-Fe-CO_3 layered double hydroxide (LDH). *Appl. Surf. Sci.* **2012**, *259*, 650-656, DOI: 10.1039/C5RA01745A.

[34] Drici, N.; Setti, N.; Jouini, Z.; Derriche, Z., Sorption study of an anionic dye benzopurpurine 4B on calcined and uncalcined Mg-Al layered double hydroxides. *J. Phys. Chem. Solids.* **2010**, *71*, 556-559, DOI: org/10.1016/j.jpcs.2009.12.035.

[35] Tran, H. N.; Lin, C. C.; Chao, H. P., Amino acids-intercalated Mg/Al layered double hydroxides as dual-electronic adsorbent for effective removal of cationic and oxyanionic metal ions. *Sep. Purif. Technol.* **2018**, *192*, 36-45, DOI: org/10.1016/j.seppur.2017.09.060.

[36] Pérez, M. R.; Pavlovic, I.; Barriga, C.; Cornejo, J.; Hermosín, M. C.; Ulibarri, M. A., Uptake of Cu^{2+}, Cd^{2+} and Pb^{2+} on Zn-Al layered double hydroxide intercalated with EDTA. *Appl. Clay Sci.* **2006**, *32*, 245-251, DOI:.org/10.1016/j.clay.2006.01.008.

[37] Yanming, S.; Dongbin, L.; Shifeng, L.; Lihui, F.; Shuai, C.; Haque, M. A., Removal of lead from aqueous solution on glutamate intercalated layered double hydroxide. *Arab. J. Chem.* **2017**, *10*, S2295-S2301, DOI:.org/10.1016/j.arabjc.2013.08.005.

[38] Pavlovic, I.; Pérez, M. R.; Barriga, C.; Ulibarri, M. A., Adsorption of Cu^{2+}, Cd^{2+} and Pb^{2+} ions by layered double hydroxides intercalated with the chelating agents diethylene triamine pentaacetate and meso-2,3-dimercaptosuccinate. *Appl. Clay Sci.* **2009**, *43*, 125-129, DOI: org/10.1016/j.clay.2008.07.020.

[39] Liang, S., Guo, X. Y., Feng, N. C., Tian, Q. H., Isotherms, kinetics and thermodynamic studies of adsorption of Cu^{2+} from aqueous solutions by

Mg^{2+}/K^{+} type orange peel adsorbents. *J. Hazard. Mater.* **2010**, *174*, 756-762, DOI: 10.1016/ j.jhazmat.2009.09.116.

[40] Deng, L.; Zhou, Si., Wang, Li.; Zhou, Sh., Fabrication of a novel $NiFe_2O_4$/Zn-Al layered double hydroxide intercalated with EDTA composite and its adsorption behavior for Cr(VI) from aqueous solution. *J. Phys. Chem. Solids.* **2017**, 104, 79-90, DOI: org/10.1016/ j.jpcs.2016.12.030.

[41] Sun, Y.; Zhou, J.; Cheng, Y.; Yu, J.; Cai, W., Hydrothermal synthesis of modified hydrophobic Zn-Al-layered double hydroxides using structure-directing agents and their enhanced adsorption capacity for p-Nitrophenol. *Adsorpt. Sci. Technol.* **2014**, *32*, 351-364, DOI:.org/10.1260%2F0263-6174.32.5.351.

[42] Xu, J.; Song, Y.; Tan, Q.; Jiang, L., Chloride absorption by nitrate, nitrite and aminobenzoate intercalated layered double hydroxides. *J. Mater. Sci.* **2017**, *52*, 5908-5916, DOI: 10.1007/s10853-017-0826-y.

[43] Liu, Q. X.; Zhou, Y. R.; Wang. M., Adsorption of methylene blue from aqueous solution onto viscose-based activated carbon fiber felts: Kinetics and equilibrium studies. *Adsorpt. Sci. Technol.* **2019**, *37*, 312-332, DOI: org/10.1177%2F0263617419827437.

[44] Citak D.; Tuzen M.; Soylak M., Simultaneous coprecipitation of lead, cobalt, copper, cadmium, iron and nickel in food samples with zirconium(IV) hydroxide prior to their flame atomic absorption spectrometric determination. *Food and Chem. Toxicol.* **2009**, *47*, 9, 2302-2307, DOI: 10.1016/ j.fct.2009.06.021.

[45] Khairul Anwar, M. S.; Nor Zakirah, I.; Ramizah Liyana, J.; Nurul Ain, M. A.; Norsuzailina, M. S.; Genevieve, G.; Rubiyah, B.; Nur Syuhada, A. Z., Application of freundlich and temkin isotherm to study the removal of Pb(II) *via* adsorption on activated carbon equipped polysulfone membrane. *Int. J. Eng. Tech.* **2018**, *7*, 91-93, DOI: 10.1021/ j100120a035 I.

[46] Koohzad, E.; Jafari, D.; Esmaeili, H., Adsorption of lead and arsenic ions from aqueous solution by activated carbon prepared from tamarix lLeaves. *Chem Select.* **2019**, *4*, 12356-12367, DOI: org/ 10.1002/slct.201903167.

[47] Foroutan, R.; Mohammadi, R.; Farjadfard, S.; Esmaeili, H.; Ramavandi, B.; Sorial, G.A., Eggshell nano-particle potential for methyl violet and mercury ion removal: Surface study and field application. *Adv Powder Technol.* **2019**, *30*, 2188-2199, DOI: org/10.1016/j.apt.2019.06.034.

[48] Nandi, B. K.; Goswami, A.; Purkait, M. K., Adsorption characteristics of brilliant green dye on kaolin. *J. Hazard. Mater.* **2009**, *161*, 387-395, DOI: 10.1016/j.jhazmat.2008.03.110.

[49] Durán, A. L.; Hernández, S. I.; Holek, I. S., Effect of surface diffusion on adsorption-desorption and catalytic kinetics in irregular Pores. II. Macro-Kinetics. *J. Phys. Chem. C.* **2017**, *121*, 27, 14557-14565, DOI:.org/10.1021/acs.jpcc.7b03653.

[50] Batool, F.; Akbar, J.; Iqbal, Sh.; Noreen, S.; Bukhari, S. N., Study of isothermal, kinetic and thermodynamic parameters for adsorption of cadmium: An overview of linear and nonlinear approach and error analysis. *Bioinorg. Chem. & Appl.* **2018**, 1-11, DOI: org/ 10.1155/2018/3463724.

[51] Doke, K. M.; Khan, M., Equilibrium, kinetic and diffusion mechanism of Cr(VI) adsorption onto activated carbon derived from wood apple shell. *Arab J. Chem.* **2017**, *10*, S252-S260, DOI: org/10.1016/ j.arabjc.2012.07.031.

[52] Kikuchi, Y.; Qian, Q.; Machida, M.; Tatsumoto, H., Effect of ZnO loading to activated carbon on Pb(II) adsorption from aqueous solution. *Carbon.* **2006**, *44*, 195-202, DOI: 10.1016/ j.carbon.2005.07.040.

[53] Akpomie, K. G.; Dawodu, F. A.; Kayode O.; Adebowale, K. O., Mechanism on the sorption of heavy metals from binary-solution by a low cost montmorillonite and its desorption potential, *Alex. Eng. J.* **2015**, *54*, 757-767, DOI: doi.org/ 10.1016/ j.aej.2015.03.025.

[54] Hu, H.; Jiang, B.; Zhang, J.; Chen, X., Adsorption of preheated ion by bio-char produced from Acidosasa edulis shoot shell in aqueous solution, *RSC Adv.* **2015**, *5*, 104769-104778, DOI: org/10.1039/C5RA20235C.

[55] Elkady, M. F.; Mahmud, M. M.; Abd-El-Rahman, M. H., Kinetic approach for cadmium sorption using

microwave synthesized nano-hydroxyapatite, *J. Non-Cryst. Solids.* **2011**, *357*, 1118-1129, DOI: org/ 10.1016/j.jnoncrysol.2010.10.021.

[56] Heidaria, A.; Younesia, H.; Mehrabanb, Z., Removal of Ni(II), Cd(II) and Pb(II) from a ternary aqueous solution by amino functionalized mesoporous and nano mesoporous silica, *Chem Eng J.* **2009**, *153*, 70-79, DOI: 10.1016/j.cej.2009.06.016.

[57] González, A. G.; Pokrovsky, O. S.; Magdalena Santana-Casiano, J.; González-Dávila, M., Bioadsorption of Heavy Metals, **2017**, DOI: 10.1007/ 978-981-10-1950-0-8.

[58] González, M. A.; Pavlovic, I.; Barriga, C., Cu(II), Pb(II) and Cd(II) sorption on different layered double hydroxides. A kinetic and thermodynamic study and competing factors. *Chem. Eng. J.* **2015**, *269*, 221-228, DOI: 10.1016/j.cej.2015.01.094.

[59] Kameda, T.; Saito, Sh.; Umetsu, Y., Mg-Al layered double hydroxide intercalated with ethylene-diaminetetraacetate anion: Synthesis and application to the uptake of heavy metal ions from an aqueous solution. *Sep. Purif. Technol.* **2005**, *47*, 20-26, DOI: org/10.1016/j.seppur.2005.06.001.

[60] Palovic, I.; Pérez, M. R.; Barriga, C.; Ulibarri, M. A.; Adsorption of Cu^{2+}, Cd^{2+} and Pb^{2+} ions by layered double hydroxides intercalated with the chelating agents diethylene tri amine penta acetate and meso-2,3-dimercaptosuccinate. *Appl Clay Sci.* **2009**, *43*, 125-129, DOI: org/10.1016/j.clay.2008.07.020.

[61] Pérez, M. R.; Pavlovic, I.; Barriga, C.; Cornejo, J.; Hermosín, M. C.; Ulibarri, M. A., Uptake of Cu^{2+}, Cd^{2+} and Pb^{2+} on Zn-Al layered double hydroxide intercalated with edta. *App. Clay Sci.* **2006**, *35*, 245-251, DOI: org/10.1016/j.clay.2006.01.008.

[62] Shan, R.; Yan, L.; Yang, K.; Hao, Y.; Du, B., Adsorption of Cd(II) by Mg-Al-CO_3- and magnetic Fe_3O_4/Mg-Al-CO_3-layered double hydroxides: Kinetic, isothermal, thermodynamic and mechanistic studies, *J Hazar Mater,* **2015**, *299*, 42-49, DOI: org/10.1016/j.jhazmat.2015.06.003.

[63] Sprynskyy, M.; Buszewski, B.; Terzyk, A. P.; Namieśnik, J., Study of the selection mechanism of heavy metal (Pb^{2+}, Cu^{2+}, Ni^{2+} and Cd^{2+}) adsorption on clinoptilolite, *J. Colloid Interface Sci.* **2006**, *304*, 21-8, DOI: org/10.1016/j.jcis.2006.07.068.

[64] Wang, C.; Wang, B.; Liu, J. T.; Yu, L.; Sun, H. W.; Wu, J., Adsorption of Cd(II) from acidic aqueous solutions by tourmaline as a novel material. *Chinese Sci Bull.* **2012**, *57*, 3218-3225, DOI: 10.1007/s11434-012-5341-6.